New York State Climate Change Projections Methodology Report

Technical Document
of the
New York State Climate Impacts Assessment

Prepared by:

Columbia University

Daniel Bader
Senior Staff Associate
Lamont-Doherty Earth Observatory
Columbia Climate School

Radley Horton
Professor of Climate
Columbia Climate School

September 2023

Contents

1. Introduction 2
2. New York State Climatology 2
   2.1. Climate Description 2
   2.2. Climate Regions and Weather Stations 7
3. Historical Analysis 9
   3.1. Trends in Annual Average Temperature 10
   3.2. Trends in Annual Precipitation 12
   3.3. Trends in Sea Level and Coastal Flooding 15
4. Climate Projections 16
   4.1. Methods 16
   4.2. Projected Mean Annual Changes 27
   4.3. Projected Changes in Extreme Events 29
5. Conclusion and Research Needs 38
6. References 39

We acknowledge Cuihua Li at the Lamont-Doherty Earth Observatory, Columbia Climate School, for her work on the historical climate data analysis and future climate projections in this report.

Preferred citation:
Bader, D., R. Horton. 2023. New York State Climate Change Projections Methodology Report. Prepared for the New York State Climate Impacts Assessment.

1. Introduction

Since the first ClimAID report in 2011, it has become clear that a changing climate is already causing major impacts in New York State. It is also now evident that if global greenhouse gas emissions are not cut dramatically, some climate change impacts in the state may exceed the capacity to adapt.

This statewide knowledge is anchored in the changes observed at global and national scales. The 2010s was the warmest decade on record globally. Since reliable recordkeeping began late in the 19th century, the warmest years globally have all occurred since 2005, with 9 of the 10 warmest years occurring since 2011 (IPCC, 2021). The year 2012 saw a record drop in summer arctic sea ice extent, far exceeding climate model projections, and 18% below the previous lowest record low in 2007 (NOAA, 2012). Recent years have seen unprecedented heat waves globally and, in the U.S., heat that has been associated with severe impacts including excess mortality of people and animals, severe forest fires, and crop losses. Meanwhile, extreme precipitation events and coastal flooding pose an increasing menace across many populous land areas globally and nationally. In 2020 alone, a record number of events (22) that caused more than a billion dollars in damages occurred (Smith, 2021). Indeed, the wave of extreme events of unprecedented frequency and intensity has helped engender a growing branch of climate science focused on attributing recent events to emissions that have already occurred (Burger et. Al 2020). It is clearer than ever that climate change and its impacts are already here.

This realization has led to new urgency to not exceed global temperature and emissions targets, such as 1.5°C (2.7°F) of global warming relative to preindustrial conditions. Warming above 1.5°C, for example, could pose an existential threat to much of the world's coral reefs and lead to irreversible changes in high-latitude regions (IPCC, 2018). A recent study found that further emissions of more than 420 $GtCO_2$—equivalent to 10 years of current emissions—would more likely than not lead to warming in excess of 1.5°C (Matthews et al. 2021). While there have been great advances in greenhouse gas emissions reductions, many spearheaded by New York State, it remains an open question whether these innovations will be fast enough to keep up with accelerating climate change impacts. It is also increasingly clear that New York State will be impacted by climate changes outside the state, through diverse mechanisms ranging from supply chain disruptions (Chee Wai and Wongsurawat, 2013), to pollution from western U.S. wildfires (Shrestha et al. 2022), to climate-influenced migration patterns (Raymond et al. 2020; Horton et al., 2021).

Section 2 of this report summarizes the climate of New York State and describes the weather stations used and regions defined in the analyses throughout this report. Section 3 is a historical analysis of climate trends for key variables, by region and station. Section 4 begins with projection methods, followed by the projections of how climate change will modify climate metrics ranging from creeping changes in time-averaged conditions to the frequency of currently rare extreme events. The final section summarizes the findings, highlights key uncertainties, and proposes topics for future work.

2. New York State Climatology

2.1. Climate Description

New York State experiences extreme geographical variations in climate due to the large latitudinal extent, elevation differences, and the influence of the Great Lakes and the Atlantic Ocean. Several climate variables are described below.

2.1.1. Average Temperature and Precipitation

The climate of New York State is best described as humid continental, with some areas of New York City and Long Island classified as humid subtropical (Peel et al., 2007). Across the state, annual average temperatures, based on the 1981–2010 climate normals, range from approximately 42°F in the northernmost areas of the state to 52°F in the New York City metropolitan region. While the southern part of New York State is the warmest on average, coastal temperatures along the immediate shoreline are moderated in summer due to the influence of sea breezes (Figure 1).

Figure 1. Annual Average Temperature for the 1981–2010 Base Period for Portions of the Northeastern United States, Including New York State

Source: NOAA, Northeast Regional Climate Center at Cornell University

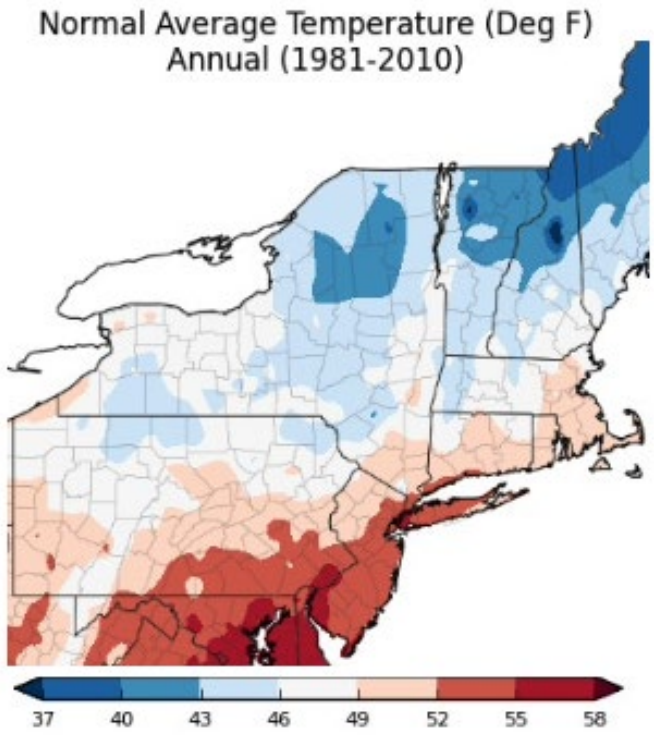

Annual precipitation is generally evenly distributed across the year in most locations in New York State. Average annual precipitation is the greatest downwind of Lake Ontario and Lake Erie due to enhanced precipitation from the Great Lakes and along the coastal plain due to the influence of coastal storms in both the warm and cool season (Figure 2). Locations in these areas average approximately 46 inches per year[1]. In the relatively drier parts of New York, which include the west-central part of the state, annual average precipitation is closer to 35 inches per year[2].

[1] Average calculated using station data from Watertown, Oswego, Buffalo, New York City, Bridgehampton, Setauket, and Dobbs Ferry.

[2] Average calculated using station data from Elmira, Ithaca, Dansville, and Rochester.

Figure 2. Average Annual Precipitation Totals for the 1981–2010 Base Period for Portions of the Northeastern United States, Including New York State

Source: NOAA, Northeast Regional Climate Center at Cornell University

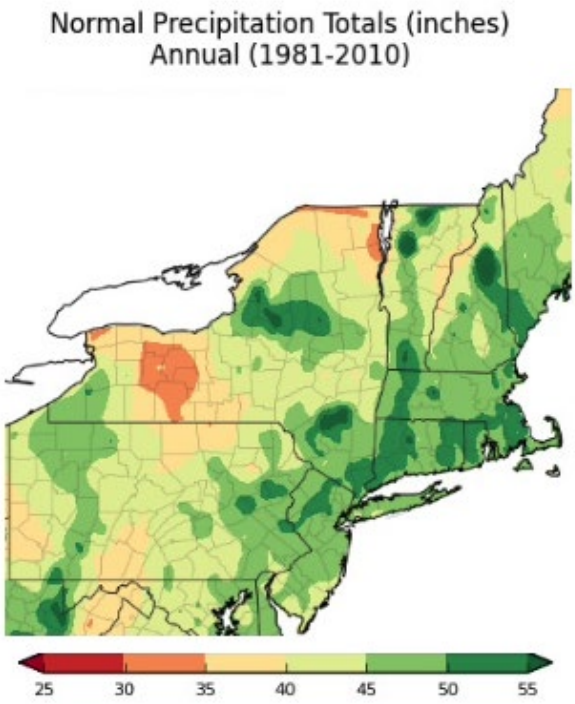

2.1.2. Snowfall

Snowfall varies dramatically across New York State based on topography and the proximity to the Great Lakes and the Atlantic Ocean (Figure 3). In parts of the Tug Hill Plateau downwind of Lake Ontario and western New York near Lake Erie, average annual snowfall exceeds 150 inches due to lake-effect snow. Closer to the coastal plain, the warming influence of the Atlantic Ocean suppresses average annual snowfall to around 30 inches.

Figure 3. Average Annual Snowfall Totals for the 1981–2010 Base Period for Portions of the Northeastern United States, Including New York State

Source: NOAA, Northeast Regional Climate Center at Cornell University

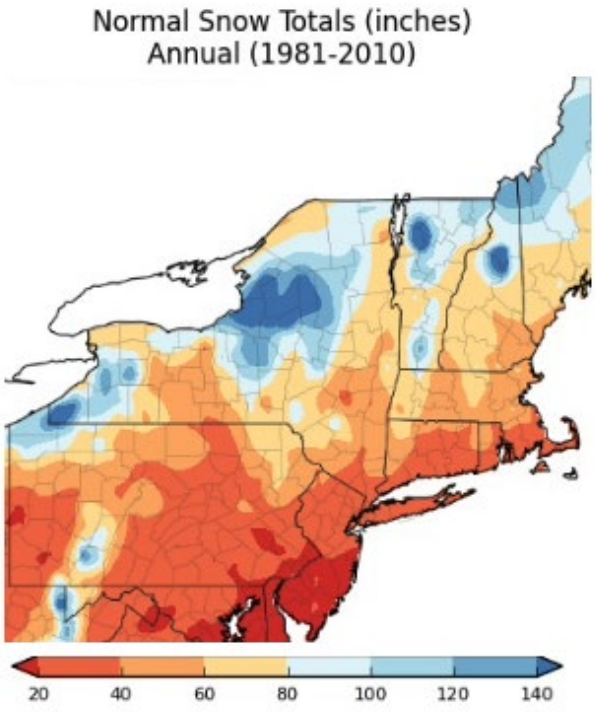

2.1.3. Extreme Events

A variety of climate extremes affect locations across New York State. These include hot and cold days, heat waves, intense precipitation, and coastal flooding caused by tropical cyclones and extratropical cyclones, including nor'easters, which are storm systems that move along the Atlantic coast and are named based on the prevailing direction of the wind flow. In all locations, the number of extreme events from year to year is highly variable.

2.1.3.1. Extreme Temperature and Heat Waves

Extreme hot days and heat waves can be defined in multiple ways to reflect the diversity of conditions experienced across the different regions in New York State. Hot days and heat waves are most common from June through August, although temperatures can exceed 90°F as early as April and as late as October. The urban heat island further elevates temperature extremes in the New York City metropolitan region and, to a lesser extent, other highly populated regions of New York State.

Specific hot-day metrics include individual days with maximum temperatures at or above thresholds such as 90°F or 95°F. For this report, heat waves are defined as three or more consecutive days with maximum temperatures at or above 90°F.

Extreme cold days are also defined to reflect the state's regional climate variations. In the coldest parts of New York State, temperatures falling below 0°F are not uncommon. Lake Placid, for example, averages 30 days below 0°F each year. Farther south, temperatures falling below 0°F are rare. Since

1900, there have been 37 days at Central Park where the minimum temperature was at or below 0°F. However, only 9 of those days have occurred within the past 60 years.

2.1.3.2. Extreme Precipitation and Flooding

Inland areas across New York experience frequent (non-snow) precipitation, with a peak in intensity in the summer. Coastal areas in New York State typically experience fewer precipitation events. However, those events are often more intense and tend to peak in the late spring as well as early fall. (Agel et al., 2015). This reflects the different mechanisms that can cause extreme precipitation, which include small-scale thunderstorms, most common in the warmer months, and large-scale coastal storms in both the warm and cool seasons.

Heavy precipitation can cause flooding in all seasons across New York State. In central and northern New York, flooding is most frequent in the spring, when rainfall and snowmelt lead to runoff. Farther south, inland flooding is more common during the summer. Larger river systems in New York State are at risk of flooding associated with the moisture from tropical cyclones. Along the coastal plain, flooding can be exacerbated by the combined effect of rainfall and coastal flooding. Urban environments face unique flood risks since the built environment limits absorption of water by underlying soils. In September 2021, deadly flooding caused by the remnants of Hurricane Ida, which produced more than 3 inches of rain at Central Park in an hour—shattering by over 50% a record set just two weeks earlier—points to the severity of the risk.

2.1.3.3. Extratropical and Tropical Cyclones

The two types of storms with the largest impact on New York State are tropical cyclones and extratropical cyclones/nor'easters. Along the coast, these storms are responsible for large storm surge events, as well as a large percentage of the occurrences of other significant impacts that can extend far inland (e.g., high winds and extreme precipitation). Mid-latitude weather systems (extratropical cyclones) can approach the state from multiple directions, causing a variety of weather events, including thunderstorms, heavy rainfall, strong winds, and frozen precipitation (e.g., snow, sleet, and freezing rain). Tropical cyclones typically approach the region from the waters to the south. However, severe impacts can extend far inland, as evidenced by recent events such as Hurricane Irene and Tropical Storm Lee in 2011, which brought heavy rainfall and flooding into inland areas of New York.

Extratropical cyclones affect the state far more frequently than tropical cyclones and are of longer duration. They generally occur in the cool season (November through April) and are associated with smaller storm surges and weaker winds along the coast as compared to the strongest tropical cyclones. Nevertheless, nor'easter flood effects can be large, since their long duration can extend the period of high winds, high water, and wave action over multiple tidal cycles. Notable recent events include a series of nor'easters in early March 2018, which brought heavy precipitation (rainfall and snowfall), high winds, and coastal flooding in consecutive events.

Landfalling tropical cyclones along the coast of New York State are uncommon, as prevailing westerly winds generally steer hurricanes away from the coast as the storms approach the northeastern United States. They generally impact the state in the warm season from July to October. The impacts of these storms are, in part, dependent on the track they take. Those that pass to the east of Long Island typically have higher wind speeds, especially for coastal locations. Those that make landfall over southeastern New York or track farther inland can produce heavy rainfall totals through central and western New York.

In July 2021, Tropical Storm Elsa made landfall over Long Island, bringing heavy rain and gusty winds to coastal locations. In late August 2021, Tropical Storm Henri made landfall in Rhode Island, and despite the center of the storm passing well to the east of New York City and Long Island, heavy rain fell across the region.

Approximately one week later in early September 2021, the remnants of Hurricane Ida brought catastrophic flooding to New York City. LaGuardia Airport and Central Park experienced 8.44 inches and 7.19 inches of rainfall from this storm, much of it falling within a matter of a few hours, with peak rainfall rates estimated between 0.08 and 0.12 inches per minute.

Prior to these recent events, the summer of 2020 saw two tropical cyclones that impacted New York State: Tropical Storm Fay and Hurricane Isaias. Before that, significant impacts occurred in 2012 from Hurricane Sandy and in 2011 from Hurricane Irene and Tropical Storm Lee.

2.1.3.4. Snowstorms

Intense lake-enhanced snowfall events occur downwind of the Great Lakes, with some storms producing up to 60 inches of snow. These events can last anywhere from a few hours to several days. Lake-effect snow is localized, and areas within miles of each other can experience large differences in snowfall totals. Locations downwind of Lake Erie and Lake Ontario experience these events most frequently, while they also occur to a lesser extent in areas in the Finger Lakes. A November 2014 event dropped over 5 feet of snow in some locations east of Buffalo (off Lake Erie), while in this same event, close to 2 feet of snow fell downwind of Lake Ontario. More recently, in late November 2022, a significant, long-duration/multi-day lake-effect event impacted locations downwind of both Lake Erie and Lake Ontario. The highest snowfall reports were from locations just south of Buffalo, with Hamburg seeing close to 80 inches of snow.

In southern parts of New York State, closer to the coastal plain, snowfall amounts occasionally exceed 20 inches during nor'easters. These events occur, on average, approximately once every 20 years. However, five of the top ten biggest snowstorms in New York City (as measured in Central Park) have occurred since 2010, with the highest total (27.5 inches) occurring on January 22–24, 2016.

2.2. Climate Regions and Weather Stations

The climate analyses and projections in this report are provided for individual regions across New York. The number of regions has expanded from seven in the prior assessment (Horton et al., 2011; 2014) to twelve, and the areas now align more closely with the U.S. Climate Divisions (Figure 4). These changes also take into consideration feedback from the Climate Needs Assessment (NYSERDA, 2020), and some modifications have been made to align regions more closely with existing boundaries (e.g., NYSDEC regions and economic development regions). The prior climate regions were constrained to county borders and while that generally remains the case here, 7 of the state's 62 counties now span multiple regions. Of the 12 regions, 5 include counties that span more than one region. The intent is to highlight that some counties encompass diverse geographies and climates, and therefore may experience varied climate change impacts. For example, parts of Essex County in the Champlain Valley may experience a different climate than areas of the county deeper within the Adirondack Mountains.

Ultimately, it is the weather stations within each region, rather than the precise boundaries and county delineations, that differentiate the 12 regional climates described here. Historical observations for a total of 27 stations across New York State were used in the historical and future analyses in this project. These stations were selected based on availability of long-term daily data and to be reflective of the

diversity of conditions across the entire state. A complete breakdown of the stations within each of the regions is shown in (Table 1). Because the available stations are not evenly distributed across the state, and due to differences in topography and proximity to water bodies, in some instances a location within one region might be best represented by a climate station from another nearby region.

Figure 4. New York State Climate Regions as Defined in this Assessment

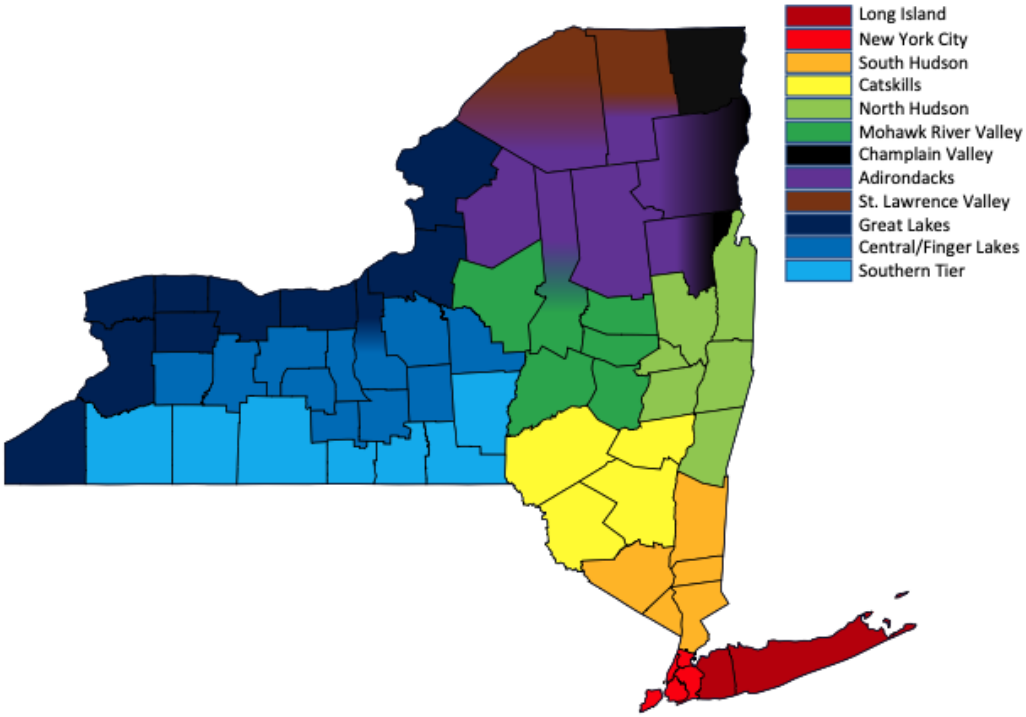

Table 1. New York State Climate Regions and Observed Weather Stations Used in Projections Analyses

Region	Observed Weather Stations
Adirondacks	Indian Lake, Lake Placid*, Wanakena,
Catskill Mountains	Mohonk*, Port Jervis
Central/Finger Lakes	Dansville, Ithaca, Syracuse*
Champlain Valley	Dannemora*

Great Lakes	Buffalo*, Fredonia*, Oswego*, Rochester*, Watertown*
Long Island	Bridgehampton*, Setauket
Mohawk River Valley	Cooperstown*
New York City	New York City/Central Park*
North Hudson River Valley	Albany*, Saratoga Springs*
Southern Tier	Alfred, Binghamton*, Elmira*, Norwich*
South Hudson River Valley	Dobbs Ferry*, Poughkeepsie
St. Lawrence River Valley	Canton*

Of the 27 stations, only a select group had sufficient data available (at the daily timescale) to complete the extreme events analysis. The * indicates that the station had sufficient data and was included in the extreme events work.

3. Historical Analysis

An analysis of historical trends in annual average temperature and precipitation was conducted for each of the 27 stations across New York State. The observed monthly data source used in this analysis is Version 2.5 of the United States Historical Climatology Network (ftp://ftp.ncdc.noaa.gov/pub/data/ushcn/v2.5, Menne et al. 2009). USHCN Version 2.5 data is constructed using a process that favors monthly data calculated directly from the latest version of the daily global historical climatology network (GHCN) data. The data are quality controlled and, if possible, adjustments are performed where inhomogeneities are identified.

The trends and their significance were computed for the 1901–2020 time period[3]. Use of a long data record helps distinguish the climate change signal associated with increasing greenhouse gas concentrations from interannual and interdecadal variability.

Trends in sea level at stations on New York's coastline are also presented.

[3] Significance of trends in annual average temperature and precipitation were computed using the Mann-Kendall test.

3.1. Trends in Annual Average Temperature

Across New York State, annual average temperatures have warmed over the past century at an average rate of approximately 0.20°F per decade (Figure 5)[4]. Over the past 40 years, annual average temperature has increased at a faster rate of 0.50°F inches per decade. All 27 stations for which the historical analysis was completed experienced warming, and 24 had trends that were significant at the 99% level over the 1901–2020 time period (see Table 2). This rate of warming across the northeastern United States over the same time period is also 0.20°F per decade. Winter warming is greatest, at a rate (0.33°F per decade) that is nearly double each of the other seasons.

Figure 5. Trend in New York State Annual Average Temperature from 1901–2020

The NOAA climate division values are weighted by area to compute the statewide average (Karl and Koss, 1984). Source: NOAA

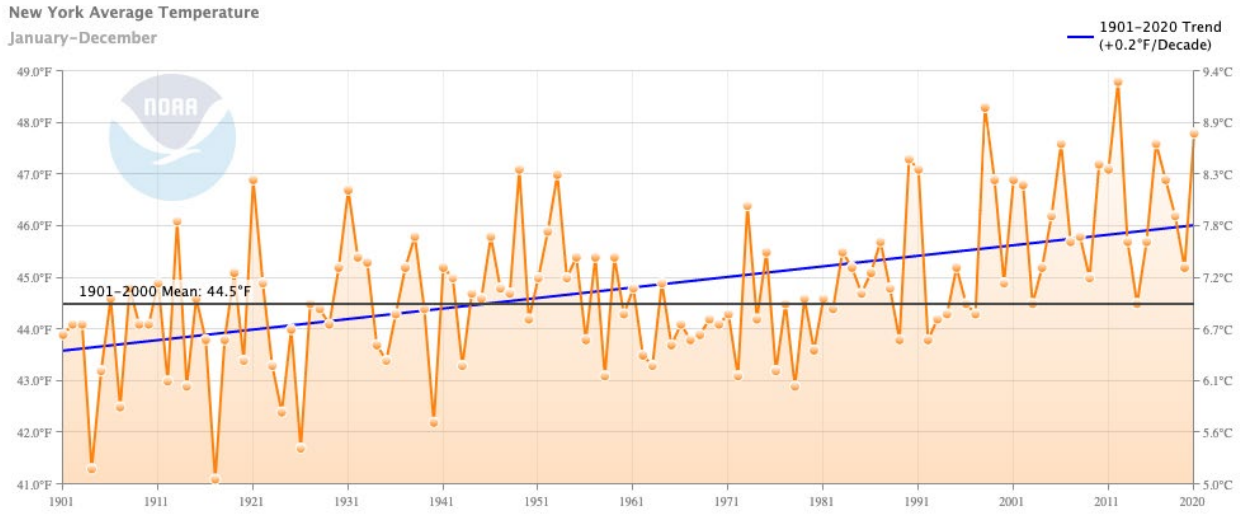

Table 2. Trends in Annual Average Temperature from 1901–2020 for Observed Weather Stations in New York State

Observed Weather Station	Temperature Trend (°F/decade)
Adirondacks – Indian Lake	0.18**
Adirondacks – Lake Placid	0.30**

[4] The trend for New York State is taken from NOAA's Climate at a Glance tool. The trend, when averaging the individual results across the 27 stations used in the analysis, is 0.23°F per decade.

Adirondacks – Wanakena	0.29**
Catskill Mountains – Mohonk	0.21**
Catskill Mountains – Port Jervis	0.35**
Central/Finger Lakes – Dansville	0.15**
Central/Finger Lakes – Ithaca	0.13**
Central/Finger Lakes – Syracuse	0.22**
Champlain Valley – Dannemora	0.34**
Great Lakes – Buffalo	0.19**
Great Lakes – Fredonia	0.11*
Great Lakes – Oswego	0.34**
Great Lakes – Rochester	0.22**
Great Lakes – Watertown	0.19**
Long Island – Bridgehampton	0.34**
Long Island – Setauket	0.36**
Mohawk River Valley – Cooperstown	0.15**
New York City – New York City/Central Park	0.34**
North Hudson River Valley – Albany	0.28**
North Hudson River Valley – Saratoga Springs	0.09

Southern Tier – Alfred	0.14**
Southern Tier – Binghamton	0.22**
Southern Tier – Elmira	0.12**
Southern Tier – Norwich	0.08
Southern Hudson River Valley – Dobbs Ferry	0.34**
Southern Hudson River Valley – Poughkeepsie	0.42**
St. Lawrence River Valley – Canton	0.24**

*Trend is significant at the 95% significance level. ** Trend is significant at the 99% significance level.

3.2. Trends in Annual Precipitation

The average rate of change for annual precipitation across New York State is an increase of approximately 0.46 inches per decade for the 1901–2020 period (Figure 6)[5]. Over the past 40 years, annual precipitation has increased at a faster rate of 1.19 inches per decade. Out of the 27 stations in New York State used for the trend analysis, 26 saw increases in annual precipitation (Table 3). Of those 26 stations that have increasing precipitation, 15 had increases that are statistically significant at the 99% level for the 1901–2020 time period. This rate of annual precipitation change is the same as the trend across the Northeast over the same time period, which is also about 0.46 inches per decade. Precipitation trends do not show significant differences among seasons.

In addition to increased annual precipitation, year-to-year precipitation variability has become more pronounced. The standard deviation of annual precipitation (a measure of variability) was greater over the 1961–2020 period compared to 1901–1960 for 24 of the 27 stations in New York State. At the state level, the increased variability is significant at the 95% level.

[5] The trend for New York State is taken from NOAA's Climate at a Glance tool. The trend when averaging the individual results across the 27 stations used in the analysis is 0.50 inches per decade.

Figure 6. Trend in New York State Average Annual Precipitation from 1901–2020

The NOAA climate division values are weighted by area to compute the statewide average (Karl and Koss, 1984). Source: NOAA

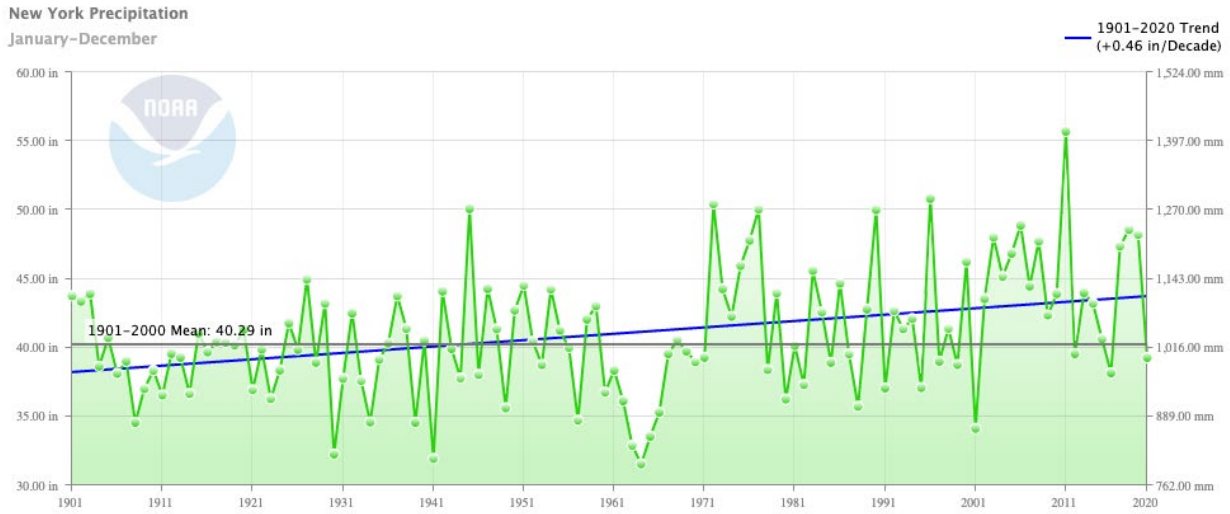

Table 3. Trends in Annual Precipitation from 1901–2020 for Observed Weather Stations in New York State

Observed Weather Station	Precipitation Trend (inches/decade)
Adirondacks – Indian Lake	0.37
Adirondacks – Lake Placid	0.45**
Adirondacks – Wanakena	0.20
Catskill Mountains – Mohonk	0.63*
Catskill Mountains – Port Jervis	0.30
Central/Finger Lakes – Dansville	0.35**
Central/Finger Lakes – Ithaca	0.55**
Central/Finger Lakes – Syracuse	0.57**

Observed Weather Station	Precipitation Trend (inches/decade)
Champlain Valley – Dannemora	0.72**
Great Lakes – Buffalo	0.88**
Great Lakes – Fredonia	0.39*
Great Lakes – Oswego	1.03**
Great Lakes – Rochester	0.40**
Great Lakes – Watertown	0.57**
Long Island – Bridgehampton	0.53**
Long Island – Setauket	-0.16
Mohawk River Valley – Cooperstown	0.34
New York City – New York City/Central Park	0.71**
North Hudson River Valley – Albany	0.88**
North Hudson River Valley – Saratoga Springs	0.59**
Southern Tier – Alfred	0.31*
Southern Tier – Binghamton	0.86**
Southern Tier – Elmira	0.60**
Southern Tier – Norwich	0.37
Southern Hudson River Valley – Dobbs Ferry	0.39

Observed Weather Station	Precipitation Trend (inches/decade)
Southern Hudson River Valley – Poughkeepsie	0.32
St. Lawrence River Valley – Canton	0.27*

*Trend is significant at the 95% significance level. ** Trend is significant at the 99% significance level.

3.3. Trends in Sea Level and Coastal Flooding

Areas on the coastal plain—defined as Long Island, New York City, lands near the southern Hudson River, and small portions of southeastern Westchester County—are at risk from rising sea levels and enhanced coastal flooding. Sea levels in coastal New York are rising at rates faster than the global average. In recent years, accelerated sea level rise globally can be attributed to the expansion of oceans as they warm and melting of land-based ice, and some studies have suggested additional local acceleration due to changing ocean currents in the Atlantic (Yin, et al. 2009; Piecuch et al., 2018). The rate of local or relative sea level rise in New York City has averaged 0.12 inches per year from 1901 to 2020 as measured by the tide gauge at the Battery. The Montauk Point station on eastern Long Island has seen sea levels rise at a rate of 0.13 inches per year for the 1947–2020 period. Both rates are nearly double the 1920–2022 mean global rate (Sweet et al., 2022), in part due to local land subsidence. This land subsidence is primarily due to local glacial isostatic adjustment, a process whereby land, once covered by or adjacent to glacial ice sheets, is still responding to the melting of that ice at the end of the last ice age. New York's coastal region, and much of the U.S. East Coast, continues to sink as land farther inland that was covered by more ice rises (Engelhart et al., 2011; Engelhart and Horton, 2012). More recently, over the past 40 years, the rate of sea level rise at the Battery has accelerated to approximately 0.17 inches per year.

Rising sea level along coastal New York State has increased the magnitude and frequency of coastal floods. In some locations, flooding now occurs at times of high astronomical tides, even in the absence of coastal storms. At the Battery, the frequency of this "nuisance flooding" (high-tide flooding) has more than doubled since the 1950s (Gornitz et al., 2019; Orton et al., 2019). When coastal storms do occur, they now flood larger areas and feature deeper—and thus more damaging and dangerous—water (Strauss et al., 2021).

Figure 7. Trend in Sea Level at the Battery, New York

Source of data: NOAA

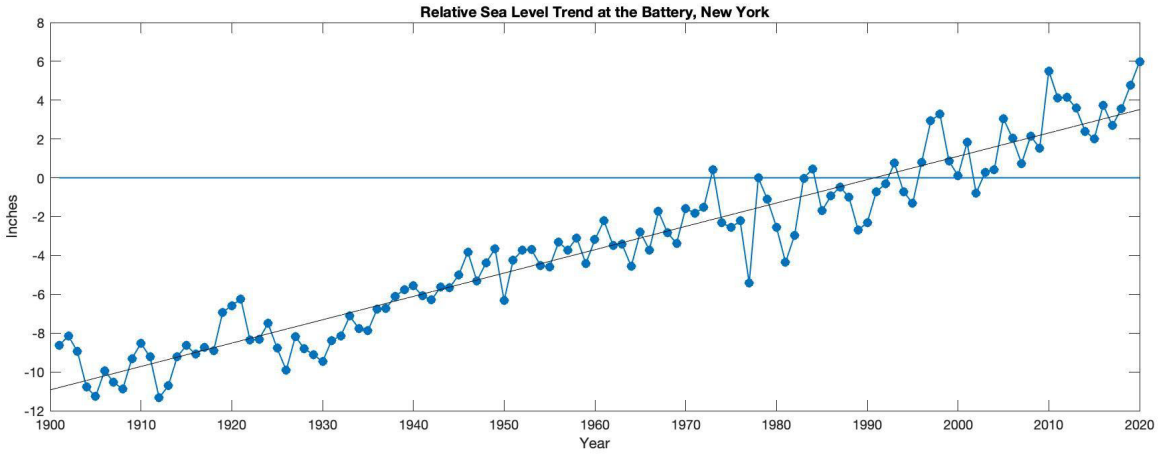

4. Climate Projections

Most of the quantitative results described below are based on the latest generation of global climate models (CMIP6) and an updated scenario framework, known as the Shared Socioeconomic Pathways (SSPs). Previous projections developed for New York State were based on CMIP5 and the RCPs or CMIP3 and SRES. In addition to modeling and methodological advances, emerging research and expanded observational data availability since the last update in 2014 have also contributed to refinements of the projections.

4.1. Methods

The global climate model (GCM) simulations for the projections in this report are from the latest iteration of the World Climate Research Programme's Coupled Model Intercomparison Project (CMIP6; https://www.wcrp-climate.org/wgcm-cmip/wgcm-cmip6) (Table 4). CMIP assesses past, present, and future climate changes from natural and anthropogenic sources by looking at a range of models (Eyring et al., 2016). The Scenario Model Intercomparison Project (ScenarioMIP) is the central CMIP6 initiative, providing multimodel climate projections based on alternative scenarios of future emissions and land-use changes produced by integrated assessment models (O'Neill et al., 2016).

Table 4. List of GCMs Used in Climate Projections

GCM Name	Monthly Temperature and Precipitation	Daily Temperature	Daily Precipitation
ACCESS-CM2	*	*	*

GCM Name	Monthly Temperature and Precipitation	Daily Temperature	Daily Precipitation
ACCESS-ESM1-5	*	*	*
AWI-CM-1-1-MR	*	*	
BCC-CSM2-MR	*	*	*
CAMS-CSM1-0	*		
CanESM5-CanOE	*		
CanESM5	*	*	*
CESM2	*		
CESM2-WACCM	*		*
CIESM	*		
CMCC-CM2-SR5	*		
CNRM-CM6-1	*	*	*
CNRM-CM6-1-HR	*		
CNRM-ESM2-1	*	*	*
EC-Earth3	*		
EC-Earth3-Veg	*		
FGOALS-g3	*		

GCM Name	Monthly Temperature and Precipitation	Daily Temperature	Daily Precipitation
FGOALS-f3-L	*		
FIO-ESM-2-0	*		
GFDL-CM4	*	*	*
GFDL-ESM4	*	*	*
GISS-E2-1-G	*		
HadGEM3-GC31-LL	*	*	*
INM-CM4-8	*	*	*
INM-CM5-0	*	*	*
IPSL-CM6A-LR	*		
KACE-1-0-G	*	*	*
MCM-UA-1-0	*		
MIROC6	*		
MPI-ESM1-2-HR	*		
MRI-ESM2-0	*		
NESM3	*		
NorESM2-LM	*	*	*

GCM Name	Monthly Temperature and Precipitation	Daily Temperature	Daily Precipitation
NorESM2-MM	*	*	*
UKESM1-0-LL	*	*	*

This project follows two prior NYSERDA projects that developed climate projections for New York State. Presented here is a brief summary of how the key components of the projections have changed over time. Maintaining consistency with prior efforts, a preference of many stakeholders across the state based on the findings of the Climate Needs Assessment (NYSERDA, 2020), is balanced with updating the climate science to ensure it aligns with cutting-edge research and national and international climate assessments (e.g., IPCC, 2021). Table 5 below demonstrates how our methodologies have stayed the same, and changed, over time. In response to stakeholder feedback focused on increasing the utility and relevance of our projections for decision-making, key advances have included increasing the number of regions in the state, providing projections centered around each decade this century, and including compound/multivariate extremes such as humidity and heat rather than focusing on single variables like temperature only. Scientific advances have also led to improved and higher-resolution climate models. Scientific advances also encouraged us to modify projection methods to assess whether some days may, for example, warm more than others, a possibility not captured by the more homogenous delta method used in prior NYSERDA assessments.

Table 5. Comparison of New York State Climate Projection Methods

	ClimAID, 2011	ClimAID Update, 2014	New York State Climate Impacts Assessment, 2023
Climate Regions and Observing Stations	7 Regions, 22 Stations	7 Regions, 7 Stations	12 Regions, 27 Stations
Baseline Years	1971–2000	1971–2000	1981–2010

	ClimAID, 2011	ClimAID Update, 2014	New York State Climate Impacts Assessment, 2023
Future Timeslices	2020s 2050s 2080s	2020s 2050s 2080s 2100	2030s 2040s 2050s 2060s 2070s 2080s 2100
Methods – Emissions Scenarios	3 SRES A1B, A2, B1	2 RCPs RCP4.5, RCP8.5	2 SSPs SSP2-4.5, SSP5-8.5
Methods – Global Climate Models (GCMs)	CMIP3 16 Global Climate Models, Monthly	CMIP5 35 Global Climate Models, Monthly	CMIP6 35 Global Climate Models, Monthly 16 Global Climate Models, Daily
Methods – Percentiles	Minimum, Central Range (16th to 83rd percentile), Maximum	Low estimate (10th percentile), Middle Range (25th to 75th percentile), High estimate (90th percentile)	Low estimate (10th percentile), Middle Range (25th to 75th percentile), High estimate (90th percentile)
Methods – Downscaling	Single gridbox, delta method used for GCM bias correction	Single gridbox, delta method used for GCM bias correction	Single gridbox, PDF fitting of changes in future minus baseline GCM in 1 percentile bins, onto observed 1 percentile bins

4.1.1. Shared Socioeconomic Pathways (SSPs)

For CMIP6, there is a new framework that has been used to design scenarios that combine socioeconomic and technological developments, known as the Shared Socioeconomic Pathways (SSPs; Raihi 2017). The SSPs are scenarios of projected socioeconomic changes across the globe through 2100 and are used to develop the emissions scenarios. The SSPs are built upon five socioeconomic development narratives: sustainable development, regional rivalry, inequality, fossil-fueled development, and middle-of-the-road development. Each SSP is consistent with multiple radiative forcing targets based on the timing that policies are implemented (during this century) at different spatial scales (Figure 8).

The ScenarioMIP experiment developed a set of nine scenarios of future greenhouse gas emissions trajectories (Gidden et al., 2019). These nine scenarios are broken down into two smaller groups: four scenarios that update the RCPs from CMIP5, achieving equivalent forcing levels of 2.5, 4.5, 6.0, and 8.5 Wm^{-2}, and five new scenarios that were not included as part of the prior RCPs. One of the new scenarios is a lower bound of 1.9 Wm^{-2} scenario, which corresponds to the most optimistic case/outcome of the Paris Climate Agreement.

This report uses two SSPs: SSP2-4.5 and SSP5-8.5. There have been some arguments made among scientists and policy makers that the greenhouse gas forcing/concentrations associated with RCP8.5 may be unrealistic. Here, we enumerate some of the reasons we chose to include these two RCPs and RCP 8.5 especially. First, these scenarios have the same end-of-century radiative forcing as the two RCPs used in previous New York State projections, providing continuity with that work. Second, they match the pathways of greatest interest to stakeholders based on the Needs Assessment responses (NYSERDA, 2020). Third, relative to many other scenarios, there were also a large number of climate models available for these two SSPs. Fourth, they span a broad range of what we consider plausible climate outcomes, including the high-consequence outcomes that are critical for risk management Wuebbles 2023). The IPCC has never assigned likelihoods to any of the RCPs, which should instead be thought of as scenarios. Fifth, while most would probably argue that the balance of evidence may suggest that lower greenhouse gas (GHG) forcing/concentrations are more likely than those associated with RCP8.5, that does not mean that the changes in extreme-event statistics, or climate impacts, associated with RCP8.5 are unrealistically high. As it becomes clearer that current climate impact models underestimate plausible high tails even when driven by only moderate GHG levels, it follows that using projections of only moderate GHG forcing would unrealistically narrow the upper bounds for the model-based distributions for impacts like heat waves and extreme precipitation.

Figure 8. Future Carbon Dioxide Emissions (from All Sources) Consistent with Five Shared Socioeconomic Pathways (SSPs)

The projections in this report are based on SSP2-4.5 and SSP5-8.5, shown in the solid lines. Source: image adapted from Riahi et al. (2017), licensed under CC BY 4.0.

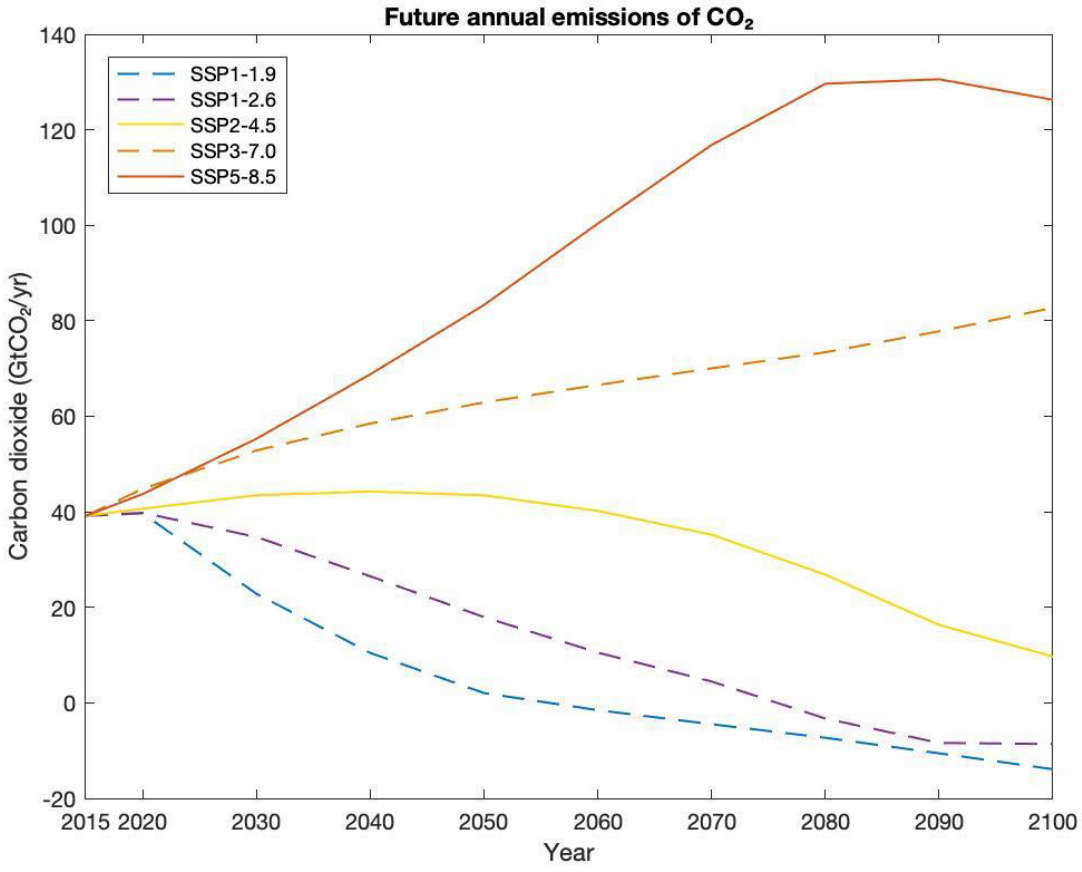

4.1.2. Mean Temperature and Precipitation Methods: Model-based Distributions

Projections for annual (as well as monthly and seasonal) average temperature and average annual (as well as monthly and seasonal) precipitation for all 27 stations were computed using 35 GCMs and two SSPs[6]. As a result of using the 35 GCMs and two SSPs, the combination produces a 70-member matrix of outputs. Keeping consistent both with the 2014 ClimAID update and stakeholder requests within New York State, results are presented across this range of outcomes at selected points in the distribution: the 10th, 25th, 75th, and 90th percentiles; the 50th percentile is also available. For each time period, the results constitute a model-based range of outcomes, which can be used to inform risk-based decision making. This approach gives equal weight to each GCM and to each of the two RCPs selected.

Mean annual temperature and precipitation projections are calculated using the delta method, used in both the 2011 and 2014 ClimAID reports. This method, which is a simple form of bias correction, compares the results for future time periods from a model to the same model's results for the baseline

[6] For all projections described in this report, only the first ensemble member/initialization was used from each GCM.

period (1981–2010). It should also be noted that geographical differences in historical climate are a much larger driver of projected geographical differences in future climate than are differential changes across regions with warming. The relatively low spatial resolution of the global climate models leads to shared grid boxes across some regions, and thus similar amounts of climate change.

4.1.3. Extreme Event Methods

For projections of extreme events, daily data from the weather stations and GCMs are used. A total of 16 models had daily data available for both SSPs at the time of analysis. Projections were developed for the 19 stations deemed to have sufficient daily data available for the 1981–2010 base period (see Table 1).

Projections of daily temperature (maximum and minimum) and precipitation were computed using a method known as quantile mapping. Quantile mapping adjusts a model value by mapping percentiles of the model's distribution onto percentiles of the observations (Cannon et al., 2015; Thrasher et al., 2012; Zhao et al., 2017). When applying a quantile-mapping-based bias correction to daily temperature extremes and daily precipitation, the approach uses a base period where both daily observations and daily GCM-simulated values are available. The quantile mapping was performed by defining the percentiles based on the entire 12-month calendar year. The analysis was run separately with percentiles defined by season, to test whether differential warming by season could skew the results if all 12 calendar months were drawn from together. Results were almost identical, and thus drawing from the full 12 months appears justified for this region.

The quantile-mapping approach in this report uses one-percentile bins in order to strike a balance between 1) capturing rich information about how baseline bias and projected change can differ across the distribution of a variable and 2) including a sufficient number of days per bin (over 100 days across the 30-year period) to minimize the role of random variability associated with small sample sizes. While more advanced downscaling techniques could in principle sample the farthest tails of the distribution, the primary impediment to improved projections of the most rare events is unrelated to downscaling and instead reflects limits to fundamental understanding—even at the largest spatial scales—of the rarest extremes. This limited understanding inevitably manifests as imperfect sampling of these events even at large spatial scales in GCMs. Bartusek et al. (2022) describe the example of the 2021 Pacific Northwest heat wave, and 2023 is sadly offering sundry examples.

For each 30-year time period, model, SSP, and station, the bias correction and downscaling approach was conducted as follows, using temperature in the illustrative example below.

Each observed day between 1981 and 2010 was assigned a temperature percentile. The same procedure was applied separately to the GCM data in the base period and in a future period. For example, if October 8, 1984, was ranked in the 33rd percentile of days for temperature in the observations, the warming experienced in the GCM at the 33rd percentile of temperatures in the two time periods (e.g., 4.0°F) was applied to the observed day. The resulting dataset can be thought of as a synthetic time series, based on the sequence of weather experienced at the station historically but modified by the amount of warming projected by each GCM in the temperature percentile associated with each day. This approach yields results that hew closely to the sequences of weather experienced over the observational period, but could underestimate the risk of sequences of events, such as a long-duration heat wave, if the observational record underestimates the true historical variability or if climate change modifies the sequences of hot days. We deem this approach superior for our application to an alternate approach—whereby the quantile bias between the GCM baseline period and observations is mapped onto the GCM future data—due to limitations in GCM ability to capture daily sequences of weather in

the region. However, to the extent that models can capture changes in sequences with climate change, the alternate approach would have merit.

The synthetic time series were then used to calculate the metrics of extreme temperatures and precipitation.

4.1.4. Downscaling and Regional Changes

The projections for each of the regions of New York State are based on the GCM output from each model's single land-based model grid box covering the center of each region. Because each GCM has a different spatial resolution, the specific coordinates of each model's grid boxes differ. Most GCMs have resolution on the order of 100km, which does not capture local processes and topography; therefore, additional analysis is needed to make the GCM data useful for local climate assessment.

Climate downscaling broadly refers to the process of using information known at large scales to make predictions at local scales. Downscaling helps to overcome the limitations of the coarse GCM resolution and can remove biases in the GCM data. There are two primary forms of downscaling. One form is dynamical downscaling, where output from the GCM is used to drive a regional climate model (RCM) at higher spatial resolution, improving the ability to simulate local processes (e.g., sea breezes) with greater detail. The other form is statistical downscaling, where a statistical relationship is established from observations between large-scale variables and a local variable. The relationship is then applied to the GCM data to obtain the localized changes from the GCM output. Hybrid approaches combining both statistical and dynamical techniques are now also being considered (Madaus et al., 2020).

As described in the earlier section, the primary method of downscaling used in this project for changes in annual average temperature and precipitation is a statistical approach known as the delta method, and the statistical method known as quantile mapping is used for projected changes in extreme events. Other statistical approaches (e.g., localized constructed analogs [LOCA]) are available and offer finer-resolution data; however, they were only beginning to be released with CMIP6 data at the time these projections were prepared.

Dynamical downscaling, using RCMs, is not employed for this update, but will ultimately have useful applications for specific climate variables of interest for New York. For example, RCMs can be used to simulate fine-scale features of the climate of New York State, including extreme heat, the urban heat island, the sea breeze, and lake-effect snow (Notaro et al., 2015; Ortiz et al., 2019).

4.1.5. Timeslices

GCMs are valuable tools for projections of the likely range of change over multidecadal time periods. These projections, known as timeslices, are expressed relative to a baseline period of 1981–2010 for temperature and precipitation. This base period has been revised since the 2014 ClimAID update to be more consistent with U.S. climate normals, NOAA's periodic update of its baseline observed climate.[7]

Projections are provided for 30-year timeslices with the time periods centered on a given decade. Thirty-year timeslices are used to provide an indication of the climate normals for those decades. By averaging over this period, much of the random year-to-year variability—or noise—is cancelled out, while the long-term influence of increasing greenhouse gases—or signal—remains.

[7] While this report was being written, NOAA updated their climate normal period to 1991–2020. The 1981–2010 period is maintained in part due to the GCM historical runs ending in 2014.

Projections are provided for each decade from the 2030s through the 2080s. (The 2020s and 2090s are excluded, as there is insufficient model output to complete a 30-year average.)[8] For certain basic quantitative projections (e.g., annual average temperature and annual precipitation) the projections are extended to 2100 using an alternate method developed for the 2014 report based on a hybrid of timeslices and earlier trend extrapolation. Please see Horton et al. (2014) for a more detailed description of this method.

4.1.6. Sea Level Rise Methods

Since the 2014 ClimAID update, there have been advances in sea level rise understanding and projection methodologies, including new approaches to capture the possibility of rapid ice melt from land-based ice sheets (Bamber et al., 2019; Gornitz et al., 2019; Fox-Kemper et al., 2021). Several recent studies confirm the plausibility of high-end sea level rise scenarios (e.g., Slangen et al., 2017) and offer techniques to adapt projections to the regional/local scale (Carson et al., 2016; Fox-Kemper et al., 2021). As noted earlier, coastal areas of New York State continue to experience faster rates of sea level rise when compared to the global average, a trend that is generally expected for the foreseeable future (Ezer, 2015).

There is growing evidence that supports the plausibility of higher-end sea level rise projections, primarily based on observations of land-based ice loss and advances in climate modeling. Probabilistic sea level rise associated with high emissions scenarios, such as those presented in Kopp et al. (2017), may represent possible future outcomes. These projections are similar to those presented in the most recent National Climate Assessment (Fourth National Climate Assessment; USGCRP, 2018) and the accompanying technical report (Sweet et al., 2017). These two studies, along with several others, informed the development of an Antarctic rapid ice melt (ARIM) scenario as part of the 2019 New York City Panel on Climate Change Report (Gornitz et al., 2019). The ARIM scenario represents a high-impact, low-probability future event. The scenario incorporates the latest science on changes in land-based ice, including glaciers, the Greenland Ice Sheet, and the Antarctic Ice Sheet.

Our report includes updated projections based on those developed for the IPCC 6th Assessment report. These projections are based on the CMIP6 models and SSP framework, and they incorporate advances in process understanding, improved and lengthened observational records, and improved ice-sheet modeling. Three scenarios used by the IPCC—SSP2-4.5-medium confidence, SSP5-8.5-medium confidence, and SSP5-8.5-low confidence—are selected for use here, since they span a broad range of plausible outcomes. For each scenario, the IPCC provides a full set of percentiles in 1% increments for tide gauges (e.g., the Battery), as well as a grid (used for Montauk Point). Because these data are available for years at the start of each decade (e.g., 2050), we interpolated the values to the middle year (e.g., 2055) of the decade to align with the 10-year timeslices previously used for sea level rise projections. Ten-year timeslices, rather than the 30-year timeslices used for other variables, are appropriate here, given the small year-to-year variability of sea level rise relative to its accelerating trend. After adjusting to the midpoint of each decade, the individual one-percentile distributions of samples for each of the three scenarios from the IPCC are combined. This results in a distribution of 297 values (3 scenarios x 99 quantiles)[9] for each location. The percentile values are taken across this distribution to form the updated sea level rise projections. These projections are provided for three

[8] The 2030s decade is the period from 2020 to 2049, the 2040s decade is the period from 2030 to 2059 . . . the 2070s decade is the period from 2060 to 2089 and the 2080s decade is the period from 2070 to 2099.

[9] The IPCC provides 107 quantiles for each scenario. This analysis removes the 0 and 100 quantiles, along with 6 other quantiles that are not full percentile values.

locations: the Battery, Montauk Point, and Albany/Troy Dam[10].

Our results also reference the higher-end ARIM scenario projection developed in 2019 for New York City. We deem this to still represent a low probability, but possible, outcome that may be worth considering in certain decision contexts, where consequences would be particularly high.

4.1.7. Differences between CMIP6 and CMIP5

The CMIP6 models have a higher spatial resolution than CMIP5; grid box sizes for many models are on the order of approximately 70 miles by 70 miles horizontally, whereas a common resolution for CMIP5 was approximately 140 miles by 140 miles. CMIP6 models also feature more advanced characterization of key system components, such as stratospheric chemistry, and more dynamic coupling across system components. The climate sensitivity—a measure of how sensitive global average temperatures are to changes in greenhouse gas concentrations—is higher in approximately one-fourth of CMIP6 models than in CMIP5 and earlier CMIP generations (Zelinka et al. 2019). Some studies (e.g., Wang et al. 2021) have argued that projections from these high-sensitivity models are less reliable than other models. The approach taken in this project, as in prior assessments, is that all models deserve equal weight. Reasons include 1) consistency with prior New York State assessment methods, 2) preference for a risk-management-based approach that produces a large range of possible outcomes rather than a best estimate, and 3) concern that models may fail to sample lower-probability, high-consequence outcomes (see Horton et al. 2011 and section 4.1.1 here for more information about the pros and cons of model weighting and the discarding of purportedly unrealistic high-end outcomes).

For the first time, the development of a comprehensive approach to sea level rise in the latest IPCC report offered the opportunity to rely on IPCC methods, rather than methods we had to generate ourselves. Therefore, there are too many differences in methodology to allow for simple explanations of why results differ from one assessment to the next. Below are key similarities and changes in sea level rise methods between this and ClimAID.

Sea level rise projections for this report incorporate the same four components as used in the 2014 ClimAID projections update: 1) sterodynamic sea level; 2) land-based ice loss from Antarctica, Greenland, and glaciers and ice caps; 3) land water storage; and 4) vertical land motion. In 2014, sea level rise was calculated as a sum of the individual components, derived from using different sources of information (e.g., set of climate models) and assumptions (e.g., for vertical land motion and ice sheet mass loss). With this method, the results were calculated at each of the percentiles of interest (and for some components, those were the only values computed or available). The distribution across the two emissions scenarios was only based on the model-based dynamic sea level and thermal expansion term. With this current update (2023), the numerical values for the full distribution for each the individual components are available from the IPCC. These projections are not the sum of the individual

[10] Projections for the Albany/Troy Dam are calculated using the data for the Battery and are adjusted for the appropriate rate of vertical land motion. The values for vertical land motion at the Battery are removed and then the local rate at the Albany/Troy Dam is added in. This is consistent with prior methods used in Horton et al. (2011 and 2014). A recent study by Parsons et al. (2023) noted that highly developed parts of New York City's coastline that are not situated on bedrock have experienced somewhat higher rates of land subsidence than used in our analysis and could continue to in the future. While these results are highly localized and neighborhood specific, rather than at the scale of our state-level analysis, they provide an example of how vulnerability can be highly concentrated spatially and why seemingly low-probability outcomes (such as very high sea level rise, very high storm surge, very severe drought, or a global financial crisis exacerbated by climate change) should never be ruled out entirely.

components at each distribution point but rather the total sea level change projection from the IPCC at that point.

4.2. Projected Mean Annual Changes

Presented here are the projected mean changes in annual average temperature, precipitation, and sea level rise. Table 6 includes results that span across all regions of New York State for average temperature and Table 7 for average precipitation. The 10th and 25th percentiles are the lowest of the 12 regional values; the 50th percentile is the average across the 12 regions; and the 75th and 90th percentiles are the highest values across the 12 regions. The projected changes in this table are representative of the direction of change and approximate order of magnitude for all regions of New York State, with some regional differences described below.

Tables of projected mean annual changes for each region can be found in the appendix to this report, including projections of monthly and seasonal changes. The ensemble average across each of the SSPs is also included in the appendix.

4.2.1. Temperature

Annual average temperatures are projected to increase across New York State by 2.5°F–4.4°F by the 2030s, 3.8°F–6.7°F by the 2050s, and 5.1°F–10.9°F by the 2080s, relative to the 1981–2010 base period.[11] Warming is projected to be greatest in the northern regions of the state. The projected changes are similar for both SSPs until approximately the 2040s, when they begin to deviate and SSP5-8.5 has greater warming for the remainder of the century. Although observed trends have shown greater winter warming than other seasons, there is too much uncertainty in the climate models to draw this conclusion for the future. For the state as a whole, projections suggest that each season will experience a comparable amount of warming in the future relative to the baseline period.

4.2.2. Precipitation

Regional annual precipitation is projected to increase by approximately 1%–8% by the 2020s, 2%–12% by the 2050s, and 6%–17% by the 2080s, relative to the 1981–2010 base period.[12] Projections show the greatest increases for areas in the southeast part of the state, although that pattern does not clearly emerge until late in the century. Although seasonal projections are less certain than annual results, the greatest increases in precipitation are projected to occur during the winter months. In the summer and fall seasons, smaller increases are generally projected. In summer, some models project reductions in precipitation.

[11] Results described in text are the middle range (25th to 75th percentile of outcomes) across the 35 GCMs and 2 SSPs. The low and high estimates (10th and 90th percentile) can be found in the appendix. These are results across all 12 regions of New York State.

[12] Results described in text are the middle range (25th to 75th percentile of outcomes) across the 35 GCMs and 2 SSPs. The low and high estimates (10th and 90th percentile) can be found in the appendix. These are results across all 12 regions of New York State.

Table 6. Projected Mean Annual Changes in Annual Average Temperature for New York State (°F)

Note: Based on 35 GCMs and two SSPs. Projections are relative to the 1981–2010 base period. Shown are the low estimate (10th percentile), middle range (25th to 75th percentile), the median (50th percentile), and high estimate (90th percentile), across all 12 regions.

	10th Percentile	25th Percentile	50th Percentile	75th Percentile	90th Percentile
2030s	+2.0°F	+2.5°F	+3.4°F	+4.4°F	+5.4°F
2050s	+2.8°F	+3.8°F	+5.3°F	+6.7°F	+8.0°F
2080s	+4.2°F	+5.1°F	+8.0°F	+10.9°F	+13.0°F
2100	+5.6°F	+5.8°F	+8.7°F	+12.5°F	+15.3°F

Table 7. Projected Changes in Annual Average Precipitation for New York State (percent)

Note: Based on 35 GCMs and two SSPs. Projections are relative to the 1981–2010 base period. Shown are the low estimate (10th percentile), middle range (25th to 75th percentile), the median (50th percentile), and high estimate (90th percentile), across all 12 regions.

	10th Percentile	25th Percentile	50th Percentile	75th Percentile	90th Percentile
2030s	-2%	+1%	+4%	+8%	+11%
2050s	-2%	+2%	+7%	+12%	+14%
2080s	+1%	+6%	+11%	+17%	+22%
2100	-4%	+4%	+11%	+21%	+30%

4.2.3. Sea Level Rise

Using the middle range (25th to 75th percentiles) across all three locations and all three scenarios, sea level is projected to rise along the New York State coastline and in the tidal Hudson by 7–12 inches by the 2030s, 12–21 inches by the 2050s, and 21–41 inches by the 2080s, relative to the 1995–2014 base period. The high-end estimate (90th percentile) for sea level rise by the 2080s is 48 inches. By 2100, sea

levels are projected to rise by as much as 69 inches (Table 8). The 10th and 25th percentiles shown in Table 8 are the lowest across all three locations, the 50th percentile is the average of all three locations, and the 75th and 90th percentiles are the highest values across the three locations. Full results for all three stations can be found in the appendix.

Based on the ARIM scenario from the 2019 New York City Panel on Climate Change report, accelerated loss of land-based ice could lead to sea level rise of up to 81 inches by the 2080s and 114 inches by 2100 under a plausible worst-case scenario. While unlikely, these projections are included here because they cannot entirely be ruled out and would have very high consequences, should they occur. Such low-probability, high-consequence scenarios may be of interest for some risk-management decisions.

Table 8. Sea Level Rise Projections for New York State (inches)

	10th Percentile	25th Percentile	50th Percentile	75th Percentile	90th Percentile	ARIM
2030s	5	7	9	12	14	
2050s	11	12	16	21	25	
2080s	18	21	30	41	48	81
2100	21	25	36	54	69	114
2150	32	41	59	94	185	

Note: Projections are shown for the low estimate (10th percentile), middle range (25th–75th percentile), the median (50th percentile), and high estimate (90th percentile), across all stations. Projections are relative to the 1995–2014 base period. These projections are based on the results from the IPCC 6th Assessment report. Also shown are the NPCC 2019 results for the Antarctic Rapid Ice Melt (ARIM) scenario. ARIM represents a physically plausible upper-end, low-probability (significantly less than 10% likelihood of occurring) scenario for the late 21st century, derived from recent modeling of ice sheet–ocean behavior. The ARIM scenario contains uncertainties stemming from incomplete knowledge of ice-sheet processes and interactions among the atmosphere, ocean, and icesheets.

Rising sea levels, absent of changes in coastal storms, will profoundly increase the frequency and extent of coastal flooding. By mid-century, some coastal and estuarine locations in New York State may experience monthly tidal flooding ("sunny day" flood events). If New York City experiences high-end sea level rise, for example, monthly tidal flooding will begin to affect coastal neighborhoods such as those surrounding Jamaica Bay by the 2050s and many other areas by the 2080s.

4.3. Projected Changes in Extreme Events

This section describes quantitative projections for events where confidence in model outputs is relatively high and qualitative projections for those types of events where uncertainties make precise

quantitative projections unwise.

4.3.1. Quantitative Changes in Extreme Events

For quantitative extremes, presented here are the results for a single station in New York State (Table 9), with full results for all stations with daily data available in the appendix. The direction of change for this location is representative of all areas across the state, while the specific number of events will vary by station due to differing baseline climate values.

Table 9. Projected Changes in Extreme Events for Dobbs Ferry, New York

Note: Projections are based on 16 GCMs (14 for heat index) and 2 SSPs and are relative to the 1981–2010 base period. Baseline data are for the 1981–2010 base period and are from the NOAA National Centers for Environmental Information (NCEI). Shown are middle range (25th to 75th percentile) of 30-year mean values from model-based outcomes. Decimal places are shown for values less than 1, although this does not indicate higher precision or certainty. Heat waves are defined as three or more consecutive days with maximum temperatures at or above 90°F. A degree day is defined as the difference between the daily average temperature and 65°F. Heating degree days occur when the daily average temperature is below 65°F, while cooling degree days occur when the daily average temperature is above 65°F. Heat index was computed using the formula from the National Weather Service.

Extreme Event	Baseline	2030s	2050s	2080s
# of days/year with maximum temperature at or above:				
90°F	18	29 to 48	41 to 64	48 to 87
95°F	4	10 to 18	13 to 29	18 to 57
# of heat waves/year	2	4 to 6	6 to 9	6 to 10
Average length of heat waves (in days)	4	5 to 5	5 to 6	5 to 8
# of days/year with heat index at or above:				
85°F	33	56 to 68	68 to 86	83 to 113
95°F	5	17 to 25	26 to 40	34 to 72

Extreme Event	Baseline	2030s	2050s	2080s
Maximum heat index	100°F	107°F to 111°F	112°F to 118°F	115°F to 130°F
Cooling Degree Days	903	1199 to 1463	1411 to 1800	1627 to 2399
# of days/year with minimum temperature at or below 32°F	105	74 to 90	54 to 82	25 to 67
# of days/year with minimum temperature at or below 0°F	0.6	0 to 0	0 to 0	0 to 0
Heating Degree Days	5181	4232 to 4536	3834 to 4234	3133 to 3883
# of days per year with precipitation exceeding:				
1 inch	15	15 to 15	15 to 17	16 to 18
2 inches	3	4 to 4	4 to 5	4 to 6
4 inches	0.2	0.2 to 0.2	0.2 to 0.2	0.2 to 0.5

4.3.1.1. Heat Waves and Cold Events

The total number of hot days in New York State is expected to increase as this century progresses. The frequency and duration of heat waves, defined as three or more consecutive days with maximum temperatures at or above 90°F, are also expected to increase. In contrast, extreme cold events, defined as the number of days per year with minimum temperature at or below 32°F and days per year with minimum temperature at or below 0°F, are expected to decrease.

4.3.1.2. Cooling and Heating Degree Days

Cooling degree days (CDD) and heating degree days (HDD) are computed by taking the daily averaged temperature and finding the departures above and below 65°F, respectively. Degree days are a measure that estimates the amount of heating or cooling needed for a building using 65°F as a baseline. Cooling degree days are used to estimate energy requirements for air conditioning, whereas heating degree days are used to estimate energy requirements for heating.

The results presented here are calculated by summing the daily values for the year and season to find the total value. Across New York State, heating degree days are projected to decrease as the century continues, while cooling degree days are projected to increase, reflecting the warming that is projected.

4.3.1.3. Heat Index

This report includes projections that measure the combined effects of high temperature and atmospheric moisture. The combination of extreme heat and humidity can lead to particularly dangerous impacts on human health, especially for vulnerable populations such as the elderly, those with certain preexisting health conditions, and those exerting themselves outdoors. Heat and humidity also lead to increased energy demand and reduced productivity. Projections are provided for the heat index, which is computed using the National Weather Service formula (Weather Prediction Center, 2022). Because of the lack of observed station data for humidity, the analysis used data from the ERA5 gridded reanalysis dataset for the calculation of historical heat index. The projections were calculated using the same methods (quantile mapping) as the other daily extreme events, using outputs from the GCMs for both temperature (daily) and humidity (changes in monthly climatology). Projections are provided for the annual maximum value of heat index and for the number of days per year with the heat index exceeding certain thresholds (e.g., days with heat index at or above 85°F and 95°F).

Across all stations in New York State, heat index values are expected to increase dramatically in the future, due in part to the nonlinear nature of the heat index, which leads to larger and larger increases in the heat index as temperatures and atmospheric moisture reach higher and higher levels.

4.3.1.4. Extreme Precipitation and Flooding

Although the percent increase in total annual precipitation is projected to be relatively small, models project somewhat larger percentage increases in the frequency of extreme precipitation events (defined as events with more than 1, 2, or 4 inches of precipitation at daily timescales). The projections for changes in extreme precipitation in New York State are consistent with global projections (Ranasinghe, 2021).

Projecting future precipitation extremes (at daily and sub-daily scales) remains a challenge. We therefore apply a hybrid approach for extreme precipitation, where we supplement the model-based quantitative projections presented earlier with qualitative projections here. One method currently being investigated relies on the relationship between temperature and water-holding capacity of the environment. The capacity increases approximately 7% for every 1°C of warming, indicating a strong potential for more intense rainfall events as the climate warms. A recent study projected changes in precipitation extremes, where the changes are proportional to the change in atmospheric moisture content near the surface (Lenderink and Attema, 2015). A similar scaling approach, using the relationship between temperature and precipitation, was considered by Zhang et al. (2017). That study found that while the relationship between water-holding capacity and temperature may be suitable for some of the midlatitudes for some applications, large uncertainties exist. Further research shows that scaling rates (the relationship between warming and moisture) differ by region, temperature, and moisture availability (Thibeault & Seth, 2014). This research found that extreme precipitation is increasing with temperature in moist, energy-limited environments, which could include the Northeast.

While the above approaches are reasonable, the possibility that the most extreme precipitation events could increase far more in intensity cannot be ruled out. Specifically, changes in atmospheric dynamics (i.e., motion in the atmosphere) could lead to stronger upward flow in convective storms, opening the door to the possibility of precipitation increases of 30%or more during the most extreme events. Some ultra-high-resolution regional climate model simulations have supported this idea (Fowler et al. 2021 and references therein). Furthermore, should troughs in the jet stream become stronger and/or locked in place more often in the future, there is the possibility that the duration of rain events could increase along with their intensity. Research on possible changes in the jet stream is continuing, with some

studies (e.g., Kornhuber et al. 2020 and Kossin, 2018) finding evidence for increased stalling and slower movement with climate change and others suggesting that any apparent trends are due more to natural variability than anthropogenic warming (e.g., Screen 2021 and Barnes and Screen 2015). Observed trends in extreme precipitation—such as the reported roughly 50%increase in daily precipitation since the middle of the 20th century over the entire Northeast—support the idea that large changes in extreme precipitation, far in excess of 7% per degree of warming, may need to be planned for. However, as noted above, the possibility that natural variability explains a sizable portion of the observed trends cannot be entirely ruled out. It is also important to note that different storm types can respond to climate change in different ways. For example, a hurricane's rainfall is driven by somewhat different mechanisms than a typical cool-season storm.

Whether or not extreme precipitation increases at a faster rate than climate models suggest, extreme riverine flooding has the potential to increase more rapidly than extreme precipitation, especially in small catchments and areas with extensive impervious surfaces, such as urban environments. While all watersheds are unique, many could be subject to changes in the timing and magnitude of peak flows due to factors other than increases in precipitation, including 1) less snow and earlier snow melt, 2) higher evapotranspiration, 3) changes in land and water management decisions, and 4) responses of vegetation to climate change. The flood threat posed by ice jams may also change in certain watersheds. Furthermore, rivers near the coast will be affected by increases in sea level and changes in storm surge. In general, local hydrological modeling may be required to tease out the relative impact of the above factors on future water availability and flood risk.

4.3.2. Qualitative Changes in Extreme Events

This section presents projections of extreme events where uncertainties make any precise quantitative projections difficult. For these events, direction of change and order of magnitude are provided, where possible. Because local projections of some of these climate extremes are challenging to make, the projections in this section are for the highest spatial resolution available, which in some cases, for example, is the northeastern United States or the North Atlantic Basin.

4.3.2.1. Extratropical Cyclones

Projecting future changes in extratropical storms remains challenging. Projections and, to a lesser extent, observations support the idea of storm tracks shifting north with climate change at a hemispheric scale, but the implications for storms in the region are less clear (Senevirate et al. 2021). In contrast, it is expected that the amount of precipitation in a storm of a given intensity will increase, with one study (Zhang & Colle, 2017) finding East Coast extratropical cyclones could become 5%–25% wetter in the future relative to present-day storms. Precipitation type (i.e., rainfall vs. frozen precipitation) associated with nor'easters is determined by air temperatures, and models project that snowstorms are expected to decrease in frequency over the coming century in a warming climate. However, this decrease is nonlinear across storm intensity. This means that while the likelihood of a given nor'easter producing snow instead of rain will decrease in the future, if atmospheric conditions are cold enough to support frozen precipitation, storms will produce more snow (or ice) than during the present day (Zarzycki, 2018).

4.3.2.2. Tropical Cyclones

Historical trends and climate model projections generally support the idea of increased tropical cyclone hazards—specifically winds and coastal and inland flooding—over New York State as the century progresses, although the random nature of individual storm tracks will continue to dominate on the decadal timescale. Confidence has grown that intense tropical cyclones of Category 3 and higher will

become more frequent in the North Atlantic, and confidence is now very high that the amount of precipitation will (on average) increase for storms of a given intensity (Seneviratne et al. 2021; Knutson et al. 2020). Both projections and historical data also show a persistent northward migration of the location of hurricane maximum intensity, increasing the chances that a hurricane exceeding Category 2 status could approach coastal New York State in the future (Kossin et al., 2017). The balance of evidence suggests that the total number of tropical cyclones in the North Atlantic will be effectively unchanged or perhaps decrease slightly (Kossin et al. 2017).

One recent study (Lee et al., 2022) focused specifically on tropical cyclones in New York State projects that storm intensity will increase by the end of the century. This same research also projects a decreasing trend in storm translation speed and increasing trend in heading, which would increase the chances of storms approaching New York from the east at slower speeds. (Lee et al., 2022) However, compared to projected changes in storm intensity and precipitation rates, these changes are less certain.

4.3.2.3. Thunderstorms

A group of studies, primarily focused on the continental United States but with some regional examples, project an increase in the atmospheric conditions favorable for severe thunderstorm development (Seeley and Romps, 2015; Diffenbaugh et al., 2013; Trapp et al., 2007). The two primary drivers are convective available potential energy (CAPE) and wind shear (Brooks et al., 2003). Research shows that both of these factors are projected to increase in the future, although the relative contribution of each to changes in the overall environment for thunderstorms remains uncertain (Seeley and Romps, 2015; Diffenbaugh et al., 2013). Trapp et al. (2007) projected changes in the number of days favorable for severe thunderstorm development for a select group of cities in the United States, including New York. This single study projected a 100% increase the number of days for New York City.

There are some studies that project increases in lightning in a warmer climate (Clark et al., 2017; Romps et al., 2014; Price and Rind, 1994). One study estimates that for each degree Celsius of warming, lightning may increase by approximately 12% in the United States (Romps et al., 2014). However, the results of more recent research, using new methods to model lightning in the future, indicate that decreases are also possible in the future (Finney et al., 2018). Therefore, it is unknown how lightning may change later in the century.

Projections of individual thunderstorms or elements within them (e.g., hail and tornadoes) remain highly uncertain.

4.3.2.4. Drought

The projected increases in average annual precipitation suggest the possibility of decreasing drought risk, but this is far from certain for multiple reasons, including the fact that there are multiple sector-specific types of drought. First, there may be large changes in the distribution of precipitation toward more-intense precipitation events, beyond the small changes suggested by GCMs. That is, movement toward larger rainfall events with fewer small events in between could imply longer dry spells that could encourage short-term (weeks to months) drought in some more vulnerable parts of the state, such as portions of the Finger Lakes region. Any tendency of the jet stream toward stronger or more prolonged ridges of high pressure—with their associated high temperatures, sunny skies, and lack of rainfall—would increase the risk of rapid-onset drought, or “flash droughts.” Second, higher average temperatures in the warm season without increases in atmospheric humidity could lead to large increases in potential evapotranspiration, meaning that more precipitation is required just to maintain the soil moisture levels associated with the previously cooler climate. Third, reductions in snow cover

associated with warming would increase flood risk in the cold season but would increase drought risk in the warm season as soils dry out earlier, potentially inducing feedbacks through warming soil temperatures as they dry, fostering further drying. To summarize, while projected increases in average annual precipitation suggest that multiyear drought risk of most interest to large municipal water managers will not increase, results for shorter term, less than one-year droughts of most import to agriculture and water supplies for smaller communities may depend on just how much summer temperatures warm as well as how quickly precipitation runs off in the future. Finally, it should be kept in mind that the 1960's drought and paleoclimate reconstructions (Pederson et al. 2013) demonstrated that, independent of climate change, a broad range of outcomes are possible in the region, even over multiyear timescales.

4.3.2.5. Snowfall

Warmer winters, a trend that has been observed in the Northeast, can mean less early-winter snowfall, more precipitation falling as rain rather than snow, and earlier snowmelt, which can affect water availability throughout the spring and summer seasons (Easterling et al., 2017, citing Notaro et al., 2014, and Demaria et al., 2016). Recent trends reveal a gradual northward migration of the average rain–snow transition zone across the United States (Easterling et al., 2017). As a result, portions of New York State could see a 10%–50% reduction in the frequency of snowfall by the end of century, under a high emissions scenario (Ning and Bradley, 2015). While projected temperature increases may reduce the likelihood of snow, future changes in frozen precipitation are also dependent upon changes in winter storm intensity and track. On balance, most of New York State is likely to see a shorter snow season, reduced snow cover and snow depth, and fewer snow events. However, for extratropical cyclones, the largest snow events of all types could grow in magnitude since a warmer atmosphere can hold more moisture.

In a warmer climate, increased water temperatures in the Great Lakes and Finger Lakes are projected to lead to delayed refreezing in fall and winter. As cold air flows over the lakes to form localized snowfall events, a longer season without ice could increase the amount of lake-effect snow, at least in the short term (Burnett et al., 2013). However, as the climate warms, the air flowing over the lakes will warm, thereby decreasing the vertical temperature gradient needed to form precipitation. High temperatures will eventually change precipitation currently falling as snow to rain in the future. It is important to note that global climate models have difficulty simulating lake-effect snow events due to their localized nature. One study found that reduced ice coverage on the lakes leads to a decrease in precipitation (Vavrus et al., 2013), and another study showed that by the middle of the century, while precipitation downwind of the lake may increase, temperatures more often may be too warm to support snowfall (Notaro et al., 2015).

4.3.2.6. Extreme Cold

Some research has raised the prospect that extreme cold-air outbreaks connected with the polar vortex, a large area of low pressure that is typically centered on the North Pole, may paradoxically become more common as high-latitude regions warm (Liu et al. 2012; Francis and Vavrus 2012). Possible changes in cold-air outbreaks remain a topic of active research (Screen et al., 2015; Lyons et al., 2018) linked to discussions about the loss of Arctic sea ice, increases in atmospheric blocking events, and changes in the jet stream (Screen and Simmonds, 2010; Liu et al. 2012; Overland et al., 2015). Increased high-latitude blocking and a more "wavy" jet stream can allow for cold air to flow down from the Arctic deep into the midlatitudes. Some research has shown that there is a relationship between the melting of sea ice and cold-weather outbreaks (Overland et al., 2015; Screen et al., 2018,) and studies have found that climate models can simulate similar results (Zhang et al., 2018). These changes are consistent with recent

observations that polar-vortex events are on the rise (Kretschmer et al., 2018). However, additional research suggests that such consistent changes in the jet stream are unlikely (e.g., Barnes and Screen, 2015). The most recent IPCC report found low confidence in the relative contribution of Arctic warming to midlatitude atmospheric changes (Doblas-Reyes et al., 2021). There is also no evidence that cold-air outbreaks in the United States have increased because of this (the polar vortex) or other phenomena (Screen et al., 2015). Furthermore, as climate change steadily increases average winter temperatures, it will become more and more difficult for even anomalously strong jet stream perturbations to yield record-breaking winter weather.

4.3.2.7. Great Lakes Water Levels and Ice Cover

Great Lakes water levels, including Lake Erie and Lake Ontario, fluctuate frequently and experience high variability at annual and sub-annual time scales. The period 1998–2013 had below-normal water levels (Assel et al., 2003), while recent years (2014–2020) have seen above-normal levels. Record-high water levels were set in the spring of 2017 for Lake Ontario and in 2018 and again in 2019 for Lake Erie.

Factors that contribute to lake levels include precipitation, runoff, and evaporation; precipitation over the lakes and runoff from the shore add to the water supply of the basin and increase water levels, while evaporation does the opposite. These processes compete with each other to influence lake levels in the absence of other non-climatic factors.

The most recent studies project increasing water levels in the Great Lakes, including Lake Erie and Lake Ontario (VanDeWeghe et al. 2022; Kayastha et al. 2022). This differs from prior modeling studies that projected slight declines by the middle to end of century in water levels, including Lake Erie and Lake Ontario (Notaro et al., 2015; Lofgren and Rouhana, 2016). These studies did indicate that slightly higher water levels are still possible in the future. Over time, research has shown that projected declines in water levels are not likely to be as great as once thought. It is also important to note that in the future, large variability at seasonal, annual, and multiyear timescales is expected to continue. These projections are thus characterized by large uncertainty, and fluctuating periods of high and low water levels are still expected in the future.

Recent trends in Great Lake ice cover show a decline in the number of days with ice cover over the past half century. For Lake Erie and Lake Ontario, the decrease in ice coverage for the 1973–2010 period was 50% and 88%, respectively (Wang et al., 2012). The shift to less ice cover has tended to occur abruptly, rather than through gradual decline (Mason et al., 2016). Lake ice coverage also experiences high variability, and year-to-year fluctuations can be high depending on environmental conditions, such as temperature and evaporation. Winter 2022–2023 saw far below normal ice coverage on both Lake Erie and Lake Ontario.

Looking into the future, continued declines in lake ice coverage are projected as temperatures warm. However, there will likely be periods of high ice coverage that deviate from the long-term downward trend. These periods are expected to coincide with winters with strong cold-air outbreaks. The recent winters of 2014 and 2019 are examples of years with very ice high cover and cold conditions. While the multiple factors that influence lake ice cover, including larger patterns of atmospheric circulation, introduce some uncertainties, on balance, ice cover is projected to continue to decrease in the future as water and air temperatures warm.

4.3.2.8. Compound Extreme Events

Compound weather or climate events are combinations of multiple climate drivers or hazards that have a larger or different impact than an individual driver or hazard would have on its own. Recent research

in this area has concentrated on both understanding the different classes or categories of compound events and investigating these specific extremes. Some studies have focused on the nonlinear impacts of compound extremes and the failure of entities to properly conceptualize and understand these complex impacts or develop resilience strategies tailored to them (Raymond et al. 2020). Some authors have considered cases in which compounding goes beyond climate hazards to include other aspects of human and natural systems (Raymond et al. 2020), such as the risk of power failures and poor air quality, both of which are correlated with extreme heat and can have serious effects on human health. Another study has categorized compound extremes into four primary categories, each of which is applicable in New York State: 1) preconditioned, 2) multivariate, 3) temporally compounding, and 4) spatially compounding (Zscheischler et al., 2020).

Preconditioned events describe when one or more hazards can cause an impact, or lead to an amplified impact, only because of a preexisting, climate-driven condition. Examples include heavy rainfall on top of snow, and false spring (when typical cold conditions return after unseasonable warmth). Rain-on-snow events are not uncommon in the Northeast (Cohen et al., 2015). Recent examples of false spring events have damaged agricultural crops and forest products in the Northeast, including maple syrup (Hufkens et al., 2012) and fruit crops (Wolfe et al., 2018).

Multivariate events refer to the co-occurrence of multiple climate drivers or hazards in the same geographical region. Examples include the combined effects of heat and humidity, or heavy rain, strong winds, and storm surge that result in flooding events during coastal storms. As an example, a paper by Coffel et al. (2017) found that under RCP 8.5, dangerous humidity and heat events in the northeastern U.S. could become approximately 30 times more common than they are today within two generations.

Temporally compounding events refer to a succession of hazards that affect a given geographical region, amplifying an impact or leading to additional impacts when compared with a single hazard. One example is a heat wave following a strong thunderstorm event that knocks out power, and therefore air conditioning. In recent years, events like this have occurred in the Mid-Atlantic, in particular in the Washington D.C., metropolitan area. This particular combination of strong storms and power outages followed by extreme heat may be of increasing concern in the future with climate change (Matthews et al., 2019). Another example is sequences of extreme winter weather, such as back-to-back nor'easters, often intertwined with extended cold-air outbreaks. Consecutive nor'easters impacted southern parts of New York State in March 2018. The consecutive nature of these storms caused prolonged periods of high tides and coastal flooding on Long Island and New York City. Locations in upstate New York experienced heavy snowfall and blizzard conditions from this same event. Such sequences can be associated with persistent troughs in the jet stream to the west and in New York State, sometimes linked physically and in popular media with the polar vortex described above.

Spatially compounding events occur when multiple connected locations are affected by the same or different hazards within a limited time window, thereby causing an impact. For example, atmospheric blocking could cause an unusually large portion of northeastern watersheds to experience heavy precipitation over the same time period, leading to nonlinear increases in riverine flood risk in New York State and beyond. In some instances, the climate extremes occurring in New York State will occur over a larger area, potentially leading indirectly to increased impacts in New York State. For example, energy demand for cooling during the more geographically expansive heat waves associated with climate change (Lyon et al., 2019) could lead to less available supply for New York State. As another example, certain configurations of the jet stream are associated with increased risk of simultaneous breadbasket crop failures, especially due to heat and drought, with implications for global food prices and food security (Kornhuber et al. 2020).

5. Conclusion and Research Needs

Across New York State, trends toward higher temperatures and more precipitation have become more robust in the decade since the first New York State climate assessment. As the availability and complexity of climate model simulations have expanded, projections for temperature and precipitation have remained relatively similar to a decade ago. It remains clear that even small increases in average temperatures will be associated with large changes in the statistics—that is, the frequency, intensity, and duration—of many types of extreme events. Across a range of variables, the upper tail of projections has grown higher in the past decade even as the lower bound has tended to remain similar.

Like all projections, these climate projections include irreducible uncertainties (Hawkins and Sutton, 2009). Sources of uncertainty include future concentrations of greenhouse gases and other forcing agents, data limitations, the random nature of some parts of the climate system, and physical system response, including but not limited to climate sensitivity as radiative forcing changes. Uncertainties associated with future greenhouse gas concentrations and physical system response dominate as the century progresses. Uncertainty is assessed using state-of-the-art climate models, multiple scenarios of future greenhouse gas concentrations, and recent peer-reviewed literature. Even so, the projections are not true probabilities, so the general range of results rather than the specific numbers should be emphasized, and the potential for outcomes outside the range presented here cannot be ruled out.

Moving forward, there is a need for further research in several areas. First and most fundamentally, more and improved observational data and modeling are essential. Additional weather stations, plus additional data sources on information like soil moisture are high priority. Higher resolution global models, as well as regional models at convection-permitting spatial scales, will also yield new insights over time. Second, a better understanding of how extreme events may change across the state is needed. While there is no single agreed upon method to achieve this, a combination of observational and modeling studies is needed focused on 1) large-scale drivers of extreme events, such as remote ocean temperature anomalies that can influence the jet stream; and 2) fine-scale processes, such as urban heat islands and convective precipitation. Third, the last decade has revealed the importance of compound extreme events, something that most assessments to date have not considered rigorously, and that has not been extensively evaluated yet for GCMs. Finally, further work is also needed on identifying climate metrics of particular use to decision-makers and those with climate impact expertise, building on but going beyond the work conducted for the 2020 NYSERDA needs assessment. Continuing to support applied climate research will ensure that climate science will continue to inform cutting-edge solutions in adaptation and greenhouse gas mitigation for New York State.

6. References

Agel, L., Barlow, M., Qian, J.-H., Colby, F., Douglas, E., & Eichler, T. (2015). Climatology of Daily Precipitation and Extreme Precipitation Events in the Northeast United States. *Journal of Hydrometeorology*, *16*(6), 2537–2557. https://doi.org/10.1175/JHM-D-14-0147.1

Assel, R. A., Quinn, F. H., & Sellinger, C. E. (2004). Hydroclimatic Factors of the Recent Record Drop in Laurentian Great Lakes Water Levels. *Bulletin of the American Meteorological Society*, *85*(8), 1143–1152. https://doi.org/10.1175/BAMS-85-8-1143

Bamber, J. L., Oppenheimer, M., Kopp, R. E., Aspinall, W. P., & Cooke, R. M. (2019). Ice sheet contributions to future sea-level rise from structured expert judgment. *Proceedings of the National Academy of Sciences*, *116*(23), 11195–11200. https://doi.org/10.1073/pnas.1817205116

Barnes, E. A., & Screen, J. A. (2015). The impact of Arctic warming on the midlatitude jet-stream: Can it? Has it? Will it? *WIREs Climate Change*, *6*(3), 277–286. https://doi.org/10.1002/wcc.337

Bartusek, S., Kornhuber, K., & Ting, M. (2022). 2021 North American heatwave amplified by climate change-driven nonlinear interactions. *Nature Climate Change*, *12*(12), 1143–1150. https://doi.org/10.1038/s41558-022-01520-4

Burger, M., Wentz, J., & Horton, R. M. (2020). The Law and Science of Climate Change Attribution. *Columbia Journal of Environmental Law*, Vol. 45 No. 1 (2020): Volume 45.1. https://doi.org/10.7916/CJEL.V45I1.4730

Burnett, A. W., Kirby, M. E., Mullins, H. T., & Patterson, W. P. (2003). Increasing Great Lake–Effect Snowfall during the Twentieth Century: A Regional Response to Global Warming? *Journal of Climate*, *16*(21), 3535–3542. https://doi.org/10.1175/1520-0442(2003)016<3535:IGLSDT>2.0.CO;2

Cannon, A. J., Sobie, S. R., & Murdock, T. Q. (2015). Bias Correction of GCM Precipitation by Quantile Mapping: How Well Do Methods Preserve Changes in Quantiles and Extremes? *Journal of Climate*, *28*(17), 6938–6959. https://doi.org/10.1175/JCLI-D-14-00754.1

Carson, M., Köhl, A., Stammer, D., A. Slangen, A. B., Katsman, C. A., W. van de Wal, R. S., Church, J., & White, N. (2016). Coastal sea level changes, observed and projected during the 20th and 21st century. *Climatic Change*, *134*(1–2), 269–281. https://doi.org/10.1007/s10584-015-1520-1

Changnon, S. A., & Karl, T. R. (2003). Temporal and Spatial Variations of Freezing Rain in the Contiguous United States: 1948–2000. *Journal of Applied Meteorology and Climatology*, *42*(9), 1302–1315. https://doi.org/10.1175/1520-0450(2003)042<1302:TASVOF>2.0.CO;2

Chee Wai, L., & Wongsurawat, W. (2013). Crisis management: Western Digital's 46-day recovery from the 2011 flood disaster in Thailand. *Strategy & Leadership*, *41*(1), 34–38. https://doi.org/10.1108/10878571311290061

Clark, S. K., Ward, D. S., & Mahowald, N. M. (2017). Parameterization-based uncertainty in future lightning flash density. *Geophysical Research Letters*, *44*(6), 2893–2901. https://doi.org/10.1002/2017GL073017

Coffel, E. D., Horton, R. M., & Sherbinin, A. de. (2017). Temperature and humidity based projections of a rapid rise in global heat stress exposure during the 21st century. *Environmental Research Letters*, *13*(1), 014001. https://doi.org/10.1088/1748-9326/aaa00e

Cohen, J., Ye, H., & Jones, J. (2015). Trends and variability in rain-on-snow events. *Geophysical Research Letters*, *42*(17), 7115–7122. https://doi.org/10.1002/2015GL065320

Demaria, E. M. C., Roundy, J. K., Wi, S., & Palmer, R. N. (2016). The Effects of Climate Change on Seasonal Snowpack and the Hydrology of the Northeastern and Upper Midwest United States. *Journal of Climate*, *29*(18), 6527–6541. https://doi.org/10.1175/JCLI-D-15-0632.1

Diffenbaugh, N. S., Scherer, M., & Trapp, R. J. (2013). Robust increases in severe thunderstorm environments in response to greenhouse forcing. *Proceedings of the National Academy of Sciences*, *110*(41), 16361–16366. https://doi.org/10.1073/pnas.1307758110

Easterling, D. R., Arnold, J. R., Knutson, T., Kunkel, K. E., LeGrande, A. N., Leung, L. R., Vose, R. S., Waliser, D. E., & Wehner, M. F. (2017). *Ch. 7: Precipitation Change in the United States. Climate Science Special Report: Fourth National Climate Assessment, Volume I*. U.S. Global Change Research Program. https://doi.org/10.7930/J0H993CC

Eyring, V., Bony, S., Meehl, G. A., Senior, C. A., Stevens, B., Stouffer, R. J., & Taylor, K. E. (2016). Overview of the Coupled Model Intercomparison Project Phase 6 (CMIP6) experimental design and organization. *Geoscientific Model Development*, *9*(5), 1937–1958. https://doi.org/10.5194/gmd-9-1937-2016

Ezer, T. (2015). Detecting Changes in the Transport of the Gulf Stream and the Atlantic Overturning Circulation from Coastal Sea Level Data: The Extreme Decline in 2009-2010 and Estimated Variations for 1935-2012. *Global and Planetary Change*, *129*. https://doi.org/10.1016/j.gloplacha.2015.03.002

Finney, D. L., Doherty, R. M., Wild, O., Stevenson, D. S., MacKenzie, I. A., & Blyth, A. M. (2018). A projected decrease in lightning under climate change. *Nature Climate Change*, *8*(3), Article 3. https://doi.org/10.1038/s41558-018-0072-6

Fowler, H. J., Lenderink, G., Prein, A. F., Westra, S., Allan, R. P., Ban, N., Barbero, R., Berg, P., Blenkinsop, S., Do, H. X., Guerreiro, S., Haerter, J. O., Kendon, E. J., Lewis, E., Schaer, C., Sharma, A., Villarini, G., Wasko, C., & Zhang, X. (2021). Anthropogenic intensification of short-duration rainfall extremes. *Nature Reviews Earth & Environment*, *2*(2), 107–122. https://doi.org/10.1038/s43017-020-00128-6

Fox-Kemper, B., Hewitt, H. T., Xiao, C., Aðalgeirsdóttir, G., Drijfhout, S. S., Edwards, T. L., Golledge, N. R., Hemer, M., Kopp, R. E., Krinner, G., Mix, A., Notz, D., Nowicki, S., Nurhati, I. S., Ruiz, L., Sallé, J.-B., Slangen, A. B. A., & Yu, Y. (2021). Ocean, Cryosphere and Sea Level Chance. In V. Masson-Delmotte, P. Zhai, A. Pirani, Connors, S.L., C. Péan, S. Berger, N. Caud, Y. Chen, L. Goldfarb, M. I. Gomis, M. Huang, K. Leitzell, E. Lonnoy, J. B. R. Matthews, T. K. Maycock, T. Waterfield, O. Yelekci, R. Yu, & B. Zhou (Eds.), *Climate Change 2021: The Physical Science Basis. Contribution of Working Group I to the Sixth Assessment Report of the Intergovernmental Panel on Climate Change.* (pp. 1211–1362). Cambridge University Press.

Francis, J. A., & Vavrus, S. J. (2012). Evidence linking Arctic amplification to extreme weather in mid-latitudes. *Geophysical Research Letters*, *39*(6). https://doi.org/10.1029/2012GL051000

Gidden, M., Riahi, K., Smith, S., Fujimori, S., Luderer, G., Kriegler, E., van Vuuren, D. P., van den Berg, M., Feng, L., Klein, D., Calvin, K., Doelman, J., Frank, S., Fricko, O., Harmsen, M., Hasegawa, T., Havlik, P., Hilaire, J., Hoesly, R., … Takahashi, K. (2019). Global emissions pathways under different socioeconomic scenarios for use in CMIP6: A dataset of harmonized emissions trajectories through the end of the century. *Geoscientific Model Development Discussions*, *12*(4), Article 4.

Gornitz, V., Oppenheimer, M., Kopp, R., Orton, P., Buchanan, M., Lin, N., Horton, R., & Bader, D. (2019). New York City Panel on Climate Change 2019 Report Chapter 3: Sea Level Rise. *Annals of the New York Academy of Sciences*, *1439*(1), 71–94. https://doi.org/10.1111/nyas.14006

Hawkins, E., & Sutton, R. (2009). The Potential to Narrow Uncertainty in Regional Climate Predictions. *Bulletin of the American Meteorological Society*, *90*(8), 1095–1108. https://doi.org/10.1175/2009BAMS2607.1

Horton, R. M., de Sherbinin, A., Wrathall, D., & Oppenheimer, M. (2021). Assessing human habitability and migration. *Science*, *372*(6548), 1279–1283. https://doi.org/10.1126/science.abi8603

Horton, R. M., Gornitz, V., Bader, D. A., Ruane, A. C., Goldberg, R., & Rosenzweig, C. (2011). Climate Hazard Assessment for Stakeholder Adaptation Planning in New York City. *Journal of Applied Meteorology and Climatology*, *50*(11), 2247–2266. https://doi.org/10.1175/2011JAMC2521.1

Hufkens, K., Friedl, M. A., Keenan, T. F., Sonnentag, O., Bailey, A., O'Keefe, J., & Richardson, A. D. (2012). Ecological impacts of a widespread frost event following early spring leaf-out. *Global Change Biology*, *18*(7), 2365–2377. https://doi.org/10.1111/j.1365-2486.2012.02712.x

IPCC. (2018). *Global warming of 1.5°C. An IPCC Special Report on the impacts of global warming of 1.5°C above pre-industrial levels and related global greenhouse gas emission pathways, in the context of strengthening the global response to the threat of climate change, sustainable development, and efforts to eradicate poverty*. Cambridge University Press.

IPCC. (2021). *Climate Change 2021: The Physical Science Basis. Contribution of Working Group I to the Sixth Assessment Report of the Intergovernmental Panel on Climate Change*. Cambridge University Press.

Karl, T., & Koss, W. J., 1931-. (1984). *Regional and national monthly, seasonal, and annual temperature weighted by area, 1895-1983* (noaa:10238). https://repository.library.noaa.gov/view/noaa/10238

Kayastha, M. B., Ye, X., Huang, C., & Xue, P. (2022). Future rise of the Great Lakes water levels under climate change. *Journal of Hydrology*, *612*, 128205. https://doi.org/10.1016/j.jhydrol.2022.128205

Knutson, T., Camargo, S. J., Chan, J. C. L., Emanuel, K., Ho, C.-H., Kossin, J., Mohapatra, M., Satoh, M., Sugi, M., Walsh, K., & Wu, L. (2020). Tropical Cyclones and Climate Change Assessment: Part II: Projected Response to Anthropogenic Warming. *Bulletin of the American Meteorological Society*, *101*(3), E303–E322. https://doi.org/10.1175/BAMS-D-18-0194.1

Kornhuber, K., Coumou, D., Vogel, E., Lesk, C., Donges, J. F., Lehmann, J., & Horton, R. M. (2020). Amplified Rossby waves enhance risk of concurrent heatwaves in major breadbasket regions. *Nature Climate Change*, *10*(1), 48–53. https://doi.org/10.1038/s41558-019-0637-z

Kossin, J. P. (2018). A global slowdown of tropical-cyclone translation speed. *Nature*, *558*(7708), 104–107. https://doi.org/10.1038/s41586-018-0158-3

Kossin, J. P., Hall, T., Knutson, T., Kunkel, K. E., Trapp, R. J., Waliser, D. E., Wehner, M. F., Wuebbles, D. J., Fahey, D. W., Hibbard, K. A., Dokken, D. J., Stewart, B. C., & Maycock, T. K. (2017). *Ch. 9: Extreme Storms. Climate Science Special Report: Fourth National Climate Assessment, Volume I*. U.S. Global Change Research Program. https://doi.org/10.7930/J07S7KXX

Kretschmer, M., Coumou, D., Agel, L., Barlow, M., Tziperman, E., & Cohen, J. (2018). More-Persistent Weak Stratospheric Polar Vortex States Linked to Cold Extremes. *Bulletin of the American Meteorological Society*, *99*(1), 49–60. https://doi.org/10.1175/BAMS-D-16-0259.1

Lee, C.-Y., Sobel, A. H., Camargo, S. J., Tippett, M. K., & Yang, Q. (2022). New York State Hurricane Hazard: History and Future Projections. *Journal of Applied Meteorology and Climatology*, *61*(6), 613–629. https://doi.org/10.1175/JAMC-D-21-0173.1

Lenderink, G., & Attema, J. (2015). A simple scaling approach to produce climate scenarios of local precipitation extremes for the Netherlands. *Environmental Research Letters*, *10*(8), 085001. https://doi.org/10.1088/1748-9326/10/8/085001

Liu, J., Curry, J. A., Wang, H., Song, M., & Horton, R. M. (2012). Impact of declining Arctic sea ice on winter snowfall. *Proceedings of the National Academy of Sciences*, *109*(11), 4074–4079. https://doi.org/10.1073/pnas.1114910109

Lofgren, B. M., & Rouhana, J. (2016). Physically Plausible Methods for Projecting Changes in Great Lakes Water Levels under Climate Change Scenarios. *Journal of Hydrometeorology*, *17*(8), 2209–2223. https://doi.org/10.1175/JHM-D-15-0220.1

Lyon, B., Barnston, A. G., Coffel, E., & Horton, R. M. (2019). Projected increase in the spatial extent of contiguous US summer heat waves and associated attributes. *Environmental Research Letters*, *14*(11), 114029. https://doi.org/10.1088/1748-9326/ab4b41

Lyons, B. A., Hasell, A., & Stroud, N. J. (2018). Enduring Extremes? Polar Vortex, Drought, and Climate Change Beliefs. *Environmental Communication*, *12*(7), 876–894. https://doi.org/10.1080/17524032.2018.1520735

Madaus, L., McDermott, P., Hacker, J., & Pullen, J. (2020). Hyper-local, efficient extreme heat projection and analysis using machine learning to augment a hybrid dynamical-statistical downscaling technique. *Urban Climate*, *32*, 100606. https://doi.org/10.1016/j.uclim.2020.100606

Mason, L. A., Riseng, C. M., Gronewold, A. D., Rutherford, E. S., Wang, J., Clites, A., Smith, S. D. P., & McIntyre, P. B. (2016). Fine-scale spatial variation in ice cover and surface temperature trends across the surface of the Laurentian Great Lakes. *Climatic Change*, *138*(1), 71–83. https://doi.org/10.1007/s10584-016-1721-2

Matthews, H. D., Tokarska, K. B., Rogelj, J., Smith, C. J., MacDougall, A. H., Haustein, K., Mengis, N., Sippel, S., Forster, P. M., & Knutti, R. (2021). An integrated approach to quantifying uncertainties in the remaining carbon budget. *Communications Earth & Environment*, *2*(1), 1–11. https://doi.org/10.1038/s43247-020-00064-9

Matthews, T., Wilby, R. L., & Murphy, C. (2019). An emerging tropical cyclone–deadly heat compound hazard. *Nature Climate Change*, *9*(8), Article 8. https://doi.org/10.1038/s41558-019-0525-6

Menne, M. J., Williams, C. N., & Vose, R. S. (2009). The U.S. Historical Climatology Network Monthly Temperature Data, Version 2. *Bulletin of the American Meteorological Society*, *90*(7), 993–1008. https://doi.org/10.1175/2008BAMS2613.1

Ning, L., & Bradley, R. S. (2015). Snow occurrence changes over the central and eastern United States under future warming scenarios. *Scientific Reports*, *5*(1), 17073. https://doi.org/10.1038/srep17073

NOAA. (2012). *Arctic sea ice: 2012 record low was 18% smaller than previous record, nearly 50 percent below average | NOAA Climate.gov*. http://www.climate.gov/news-features/featured-images/arctic-sea-ice-2012-record-low-was-18-smaller-previous-record-nearly

Notaro, M., Bennington, V., & Lofgren, B. (2015). Dynamical Downscaling–Based Projections of Great Lakes Water Levels. *Journal of Climate*, *28*(24), 9721–9745. https://doi.org/10.1175/JCLI-D-14-00847.1

Notaro, M., Bennington, V., & Vavrus, S. (2015). Dynamically Downscaled Projections of Lake-Effect Snow in the Great Lakes Basin*,+. *Journal of Climate*, *28*(4), 1661–1684. https://doi.org/10.1175/JCLI-D-14-00467.1

NYSERDA. (2020). *Climate Needs Assessment for New York State*. New York State Energy Research and Development Authority (NYSERDA). https://www.nyserda.ny.gov/-/media/Project/Nyserda/Files/Publications/Research/Environmental/20-31-Climate-Needs-Assessment-for-New-York-State.pdf

O'Neill, B. C., Tebaldi, C., van Vuuren, D. P., Eyring, V., Friedlingstein, P., Hurtt, G., Knutti, R., Kriegler, E., Lamarque, J.-F., Lowe, J., Meehl, G. A., Moss, R., Riahi, K., & Sanderson, B. M. (2016). The Scenario Model Intercomparison Project (ScenarioMIP) for CMIP6. *Geoscientific Model Development*, *9*(9), 3461–3482. https://doi.org/10.5194/gmd-9-3461-2016

Ortiz, L. E., González, J. E., Horton, R., Lin, W., Wu, W., Ramamurthy, P., Arend, M., & Bornstein, R. D. (2019). High-resolution projections of extreme heat in New York City. *International Journal of Climatology*, *39*(12), 4721–4735. https://doi.org/10.1002/joc.6102

Orton, P. M., Lin, N., Gornitz, V., Colle, B., Booth, J., Feng, K., Buchanan, M., Oppenheimer, M., & Patrick, L. (2019). New York City Panel on Climate Change 2019 Report Chapter 4: Coastal Flooding. *Annals of the New York Academy of Sciences*, *1439*(1), 95–114. https://doi.org/10.1111/nyas.14011

Overland, J., Francis, J. A., Hall, R., Hanna, E., Kim, S.-J., & Vihma, T. (2015). The Melting Arctic and Midlatitude Weather Patterns: Are They Connected?*. *Journal of Climate*, *28*(20), 7917–7932. https://doi.org/10.1175/JCLI-D-14-00822.1

Parsons, T., Wu, P., (Matt) Wei, M., & D'Hondt, S. (2023). The Weight of New York City: Possible Contributions to Subsidence From Anthropogenic Sources. *Earth's Future*, *11*(5), e2022EF003465. https://doi.org/10.1029/2022EF003465

Pederson, N., Bell, A. R., Cook, E. R., Lall, U., Devineni, N., Seager, R., Eggleston, K., & Vranes, K. P. (2013). Is an Epic Pluvial Masking the Water Insecurity of the Greater New York City Region?*,+. *Journal of Climate*, *26*(4), 1339–1354. https://doi.org/10.1175/JCLI-D-11-00723.1

Peel, M. C., Finlayson, B. L., & McMahon, T. A. (2007). Updated world map of the Köppen-Geiger climate classification. *Hydrology and Earth System Sciences*, *11*(5), 1633–1644. https://doi.org/10.5194/hess-11-1633-2007

Piecuch, C. G., Huybers, P., Hay, C. C., Kemp, A. C., Little, C. M., Mitrovica, J. X., Ponte, R. M., & Tingley, M. P. (2018). Origin of spatial variation in US East Coast sea-level trends during 1900–2017. *Nature*, *564*(7736), 400–404. https://doi.org/10.1038/s41586-018-0787-6

Price, C., & Rind, D. (1994). Modeling Global Lightning Distributions in a General Circulation Model. *Monthly Weather Review*, *122*(8), 1930–1939. https://doi.org/10.1175/1520-0493(1994)122<1930:MGLDIA>2.0.CO;2

Ranasignhe, R., Ruane, A. C., Vautard, R., Arnell, N., Coppola, E., Cruz, A., Dessai, S., Islam, A. S., Rahimi, M., Ruiz Carrascal, D., Sillmann, J., Sylla, M. B., Tebaldi, C., Wang, W., & Zaaboul, R. (2021). Climate Change Information for Regional Impact and for Risk Assessment. In V. Masson-Delmotte, P. Zhai, A. Pirani, Connors, S., C. Pean, S. Berger, N. Caud, L. Chen, L. Goldfarb, M. I. Gomis, M. Huang, K. Leitzell, E. Lonnoy, J. B. R. Matthews, T. K. Maycock, T. Waterfield, O. Yelekci, R. Yu, & B. Zhou (Eds.), *Climate Change 2021: The Physical Science Basis. Contribution of Working Group I to the Sixth Assessment Report of the Intergovernmental Panel on Climate Change*. Cambridge University Press.

Raymond, C., Horton, R. M., Zscheischler, J., Martius, O., AghaKouchak, A., Balch, J., Bowen, S. G., Camargo, S. J., Hess, J., Kornhuber, K., Oppenheimer, M., Ruane, A. C., Wahl, T., & White, K. (2020). Understanding and managing connected extreme events. *Nature Climate Change*, *10*(7), 611–621. https://doi.org/10.1038/s41558-020-0790-4

Riahi, K., van Vuuren, D. P., Kriegler, E., Edmonds, J., O'Neill, B. C., Fujimori, S., Bauer, N., Calvin, K., Dellink, R., Fricko, O., Lutz, W., Popp, A., Cuaresma, J. C., Kc, S., Leimbach, M., Jiang, L., Kram, T., Rao, S., Emmerling, J., … Tavoni, M. (2017). The Shared Socioeconomic Pathways and their energy, land use, and greenhouse gas emissions implications: An overview. *Global Environmental Change*, *42*, 153–168. https://doi.org/10.1016/j.gloenvcha.2016.05.009

Romps, D. M., Seeley, J. T., Vollaro, D., & Molinari, J. (2014). Projected increase in lightning strikes in the United States due to global warming. *Science*, *346*(6211), 851–854. https://doi.org/10.1126/science.1259100

Screen, J. A. (2021). An ice-free Arctic: What could it mean for European weather? *Weather*, *76*(10), 327–328. https://doi.org/10.1002/wea.4069

Screen, J. A., Bracegirdle, T. J., & Simmonds, I. (2018). Polar Climate Change as Manifest in Atmospheric Circulation. *Current Climate Change Reports*, *4*(4), 383–395. https://doi.org/10.1007/s40641-018-0111-4

Screen, J. A., Deser, C., & Sun, L. (2015). Reduced Risk of North American Cold Extremes due to Continued Arctic Sea Ice Loss. *Bulletin of the American Meteorological Society*, *96*(9), 1489–1503. https://doi.org/10.1175/BAMS-D-14-00185.1

Screen, J. A., & Simmonds, I. (2010). The central role of diminishing sea ice in recent Arctic temperature amplification. *Nature*, *464*(7293), 1334–1337. https://doi.org/10.1038/nature09051

Seeley, J. T., & Romps, D. M. (2015). The Effect of Global Warming on Severe Thunderstorms in the United States. *Journal of Climate*, *28*(6), 2443–2458. https://doi.org/10.1175/JCLI-D-14-00382.1

Seneviratne, S. I., Zhang, X., Adnan, M., Badi, W., Dereczynski, C., Di Luca, A., Ghosh, S., Iskandar, I., Kossin, J., Lewis, S., Otto, F., Pinto, I., Satoh, M., Vincente-Serrano, S. M., Wehner, M., & Zhou, B. (2021). Weather and Climate Extreme Events in a Changing Climate. In V. Masson-Delmotte, P. Zhai, A. Pirani, Connors, S., C. Pean, S. Berger, N. Caud, L. Chen, L. Goldfarb, M. I. Gomis, M. Huang, K. Leitzell, E. Lonnoy, J. B. R. Matthews, T. K. Maycock, T. Waterfield, O. Yelekci, R. Yu, & B. Zhou (Eds.), *Climate Change 2021: The Physical Science Basis. Contribution of Working Group I to the Sixth Assessment Report of the Intergovernmental Panel on Climate Change*. Cambridge University Press.

Shrestha, B., Brotzge, J. A., & Wang, J. (2022). Observations and Impacts of Long-Range Transported Wildfire Smoke on Air Quality Across New York State During July 2021. *Geophysical Research Letters*, *49*(19), e2022GL100216. https://doi.org/10.1029/2022GL100216

Slangen, A., van de Wal, R., Reerink, T., de Winter, R., Hunter, J., Woodworth, P., & Edwards, T. (2017). The Impact of Uncertainties in Ice Sheet Dynamics on Sea-Level Allowances at Tide Gauge Locations. *Journal of Marine Science and Engineering*, *5*(2), 21. https://doi.org/10.3390/jmse5020021

Smith, A. B. (2021). *U.S. Billion-dollar Weather and Climate Disasters, 1980—Present (NCEI Accession 0209268)* [dataset]. NOAA National Centers for Environmental Information. https://doi.org/10.25921/STKW-7W73

Strauss, B. H., Orton, P. M., Bittermann, K., Buchanan, M. K., Gilford, D. M., Kopp, R. E., Kulp, S., Massey, C., Moel, H. de, & Vinogradov, S. (2021). Economic damages from Hurricane Sandy attributable to sea level rise caused by anthropogenic climate change. *Nature Communications*, *12*(1), 2720. https://doi.org/10.1038/s41467-021-22838-1

Sweet, W. V., Kopp, R. E., Weaver, J., Obeysekera, J., Horton, R. M., Thieler, E. R., & Zervas, C. (2017). *Global and Regional Sea Level Rise Scenarios for the United States.* (083; NOAA Technical Report NOS CO-OPS). NOAA/NOS Center for Operational Oceanographic Products and Services.

Thibeault, J. M., & Seth, A. (2014). Changing climate extremes in the Northeast United States: Observations and projections from CMIP5. *Climatic Change*, *127*(2), 273–287. https://doi.org/10.1007/s10584-014-1257-2

Thrasher, B., Maurer, E. P., McKellar, C., & Duffy, P. B. (2012). Technical Note: Bias correcting climate model simulated daily temperature extremes with quantile mapping. *Hydrology and Earth System Sciences*, *16*(9), 3309–3314. https://doi.org/10.5194/hess-16-3309-2012

Trapp, R. J., Diffenbaugh, N. S., Brooks, H. E., Baldwin, M. E., Robinson, E. D., & Pal, J. S. (2007). Changes in severe thunderstorm environment frequency during the 21st century caused by anthropogenically enhanced global radiative forcing. *Proceedings of the National Academy of Sciences*, *104*(50), 19719–19723. https://doi.org/10.1073/pnas.0705494104

USGCRP. (2018_: Impacts, Risks, and Adaptation in the United States: Fourth National Climate Assessment, Volume II [Reidmiller, D.R., C.W. Avery, D.R. Easterling, K.E. Kunkel, K.L.M. Lewis, T.K. Maycock, and B.C. Stewart (eds.)]. U.S. Global Change Research Program, Washington, DC, USA, 1515 pp. https://doi.org/10.7930/NCA4.2018

VanDeWeghe, A., Lin, V., Jayaram, J., & Gronewold, A. D. (2022). Changes in Large Lake Water Level Dynamics in Response to Climate Change. *Frontiers in Water*, *4*, 805143. https://doi.org/10.3389/frwa.2022.805143

Vavrus, S., Notaro, M., & Zarrin, A. (2013). The Role of Ice Cover in Heavy Lake-Effect Snowstorms over the Great Lakes Basin as Simulated by RegCM4. *Monthly Weather Review*, *141*(1), 148–165. https://doi.org/10.1175/MWR-D-12-00107.1

Wang, C., Soden, B. J., Yang, W., & Vecchi, G. A. (2021). Compensation Between Cloud Feedback and Aerosol-Cloud Interaction in CMIP6 Models. *Geophysical Research Letters*, *48*(4). https://doi.org/10.1029/2020GL091024

Wang, J., Bai, X., Hu, H., Clites, A., Colton, M., & Lofgren, B. (2012). Temporal and Spatial Variability of Great Lakes Ice Cover, 1973–2010. *Journal of Climate*, *25*(4), 1318–1329. https://doi.org/10.1175/2011JCLI4066.1

Weather Prediction Center. (2022). *Heat Index Equation*. https://www.wpc.ncep.noaa.gov/html/heatindex_equation.shtml

Wolfe, D. W., DeGaetano, A. T., Peck, G. M., Carey, M., Ziska, L. H., Lea-Cox, J., Kemanian, A. R., Hoffmann, M. P., & Hollinger, D. Y. (2018). Unique challenges and opportunities for northeastern US crop production in a changing climate. *Climatic Change*, *146*(1–2), 231–245. https://doi.org/10.1007/s10584-017-2109-7

Wuebbles, D. J. (2023). Can Global Mean Temperatures be Held to 1.5 ° C or Less without Major Efforts in Carbon Removal / Geoengineering? *Journal of Climate Action, Research, and Policy*, S2972312423500017. https://doi.org/10.1142/S2972312423500017

Yin, J., Schlesinger, M. E., & Stouffer, R. J. (2009). Model projections of rapid sea-level rise on the northeast coast of the United States. *Nature Geoscience*, *2*(4), 262–266. https://doi.org/10.1038/ngeo462

Zarzycki, C. M. (2018). Projecting Changes in Societally Impactful Northeastern U.S. Snowstorms. *Geophysical Research Letters*, *45*(21), 12,067-12,075. https://doi.org/10.1029/2018GL079820

Zelinka, M. D., Myers, T. A., McCoy, D. T., Po-Chedley, S., Caldwell, P. M., Ceppi, P., Klein, S. A., & Taylor, K. E. (2020). Causes of Higher Climate Sensitivity in CMIP6 Models. *Geophysical Research Letters*, *47*(1). https://doi.org/10.1029/2019GL085782

Zhang, P., Wu, Y., Simpson, I. R., Smith, K. L., Zhang, X., De, B., & Callaghan, P. (2018). A stratospheric pathway linking a colder Siberia to Barents-Kara Sea sea ice loss. *Science Advances*, *4*(7), eaat6025. https://doi.org/10.1126/sciadv.aat6025

Zhang, X., Zwiers, F. W., Li, G., Wan, H., & Cannon, A. J. (2017). Complexity in estimating past and future extreme short-duration rainfall. *Nature Geoscience; London*, *10*(4), 255–259. http://dx.doi.org.ezproxy.cul.columbia.edu/10.1038/ngeo2911

Zhang, Z., & Colle, B. A. (2017). Changes in Extratropical Cyclone Precipitation and Associated Processes during the Twenty-First Century over Eastern North America and the Western Atlantic Using a Cyclone-Relative Approach. *Journal of Climate*, *30*(21), 8633–8656. https://doi.org/10.1175/JCLI-D-16-0906.1

Zhao, T., Bennett, J. C., Wang, Q. J., Schepen, A., Wood, A. W., Robertson, D. E., & Ramos, M.-H. (2017). How Suitable is Quantile Mapping For Postprocessing GCM Precipitation Forecasts? *Journal of Climate*, *30*(9), 3185–3196. https://doi.org/10.1175/JCLI-D-16-0652.1

Zscheischler, J., Martius, O., Westra, S., Bevacqua, E., Raymond, C., Horton, R. M., van den Hurk, B., AghaKouchak, A., Jézéquel, A., Mahecha, M. D., Maraun, D., Ramos, A. M., Ridder, N. N., Thiery, W., & Vignotto, E. (2020). A typology of compound weather and climate events. *Nature Reviews Earth & Environment*, *1*(7), Article 7. https://doi.org/10.1038/s43017-020-0060-z